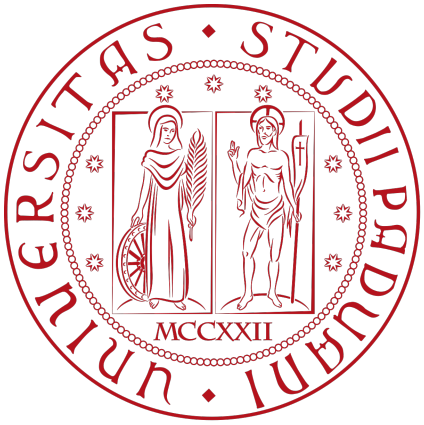
UNIVERSITÀ DEGLI STUDI DI PADOVA

DIPARTIMENTO DI BIOLOGIA

Corso di Laurea in Biologia Molecolare



ELABORATO DI LAUREA

La piccola molecola PS10 inibisce la replicazione del Virus della Sindrome Riproduttiva e Respiratoria Suina (PRRSV) mediante il targeting di HSP90 e molteplici proteine virali non strutturali

Tutor
Prof.ssa Maria Cristina Parolin
Dipartimento di Medicina Molecolare

Laureanda: *Arianna Momesso*

ANNO ACCADEMICO 2025/2026

Indice

Abstract

1 Stato dell'arte: introduzione al problema biologico 1
1.1 PRRSV: il Virus della Sindrome Riproduttiva e Respiratoria Suina . . . 1
1.1.1 Classificazione e genoma . . . 1
1.1.2 Replicazione . . . 2
1.2 PS10 come composto antivirale . . . 3

2 Approccio sperimentale: materiali e metodi 4
2.1 Cellule e virus . . . 4
2.2 Reagenti e anticorpi . . . 4
2.3 Saggio di citotossicità . . . 5
2.4 Estrazione di RNA e RT-qPCR . . . 5
2.5 Western blotting . . . 5
2.6 Immunofluorescenza indiretta (IFA) . . . 5
2.7 Titolazione virale mediante saggio delle placche . . . 6
2.8 Interazione diretta PRRSV - PS10 . . . 6
2.9 Trasfezione . . . 6
2.10 Cellular Thermal Shift Assay (CETSA) . . . 7
2.11 Docking molecolare . . . 7
2.12 Analisi statistica . . . 7

3 Risultati e discussione 7
3.1 PS10 inibisce la replicazione di PRRSV in cellule epiteliali renali di scimmia (Marc-145) e in macrofagi alveolari suini (PAMs) . 7
3.2 Attività anti-PRRSV di PS10 in condizioni di diversi regimi di trattamento . . . 10
3.3 PS10 non stabilisce una interazione diretta con la particella virale 11
3.4 Attività anti-PRRSV di PS10 nei confronti di diversi ceppi virali 12
3.5 Inibizione specifica di PS10 a livello della fase di replicazione virale . . . 13
3.6 PS10 riduce la produzione di citochine pro-infiammatorie mediante down-regolazione dell'espressione di HSP90 . . . 14
3.7 PS10 riduce l'espressione delle proteine virali nsp2, nsp3, nsp10 e nsp11 . . . 18
3.8 Interazione tra PS10 e le proteine virali nsp1, nsp3, nsp10 e nsp11 19

4 Considerazioni e conclusione 20

5 Bibliografia 23

6 Appendice (articolo)

Abstract

Il Virus della Sindrome Riproduttiva e Respiratoria Suina (PRRSV) rappresenta una grave minaccia per la zootecnia e la sicurezza alimentare globale. A causa dell'elevata variabilità genetica del virus e della limitata protezione offerta dagli attuali vaccini, emerge la necessità urgente di sviluppare nuovi e più efficaci trattamenti antivirali.

Il presente studio propone un'analisi approfondita sull'efficacia del composto 2-[(2,4diidrossifenil)solfonil]isoindolina-4,6-diolo (noto come PS10) come inibitore della replicazione virale [1]. Gli autori hanno indagato il duplice meccanismo d'azione del PS10: da un lato, è stata analizzata la sua capacità di sopprimere l'espressione della proteina da shock termico 90 (HSP90) indotta dal virus, ostacolando così la diffusione virale e attenuando la produzione di citochine pro-infiammatorie; dall'altro, è stata esaminata l'interazione diretta di PS10 con specifiche proteine virali non strutturali (nsp2, nsp3, nsp10 e nsp11), supportata da test di docking molecolare e Cellular Thermal Shift Assay (CETSA).

I risultati evidenziano come la modulazione dei fattori dell'ospite e il targeting delle proteine virali rappresentino una combinazione sinergica altamente efficace in ambito terapeutico. Inoltre, l'analisi sottolinea il notevole potenziale del PS10 nello sviluppo di terapie antivirali ad ampio spettro, aprendo nuove prospettive per il controllo delle infezioni da PRRSV.

1 Stato dell'arte: introduzione al problema biologico

1.1 PRRSV: il Virus della Sindrome Riproduttiva e Respiratoria Suina

Il Virus della Sindrome Riproduttiva e Respiratoria Suina (PRRSV), agente eziologico della PRRS, causa una delle patologie suinicole a maggior impatto globale. Questo patogeno persistente mostra uno stretto tropismo tissutale, infettando preferenzialmente la linea monocitica suina e in particolare i macrofagi alveolari (PAMs), sebbene *in vitro* replichi anche su linee renali di scimmia verde africana (MA-104 e la derivata Marc-145).
Emersa tra Europa e Nord America a fine anni '80 come malattia "misteriosa" [2], la PRRS si manifesta clinicamente con un grave distress respiratorio nei suinetti e un severo fallimento riproduttivo nelle scrofe gravide, caratterizzato da aborti e feti mummificati o nati morti.

Le analisi molecolari hanno identificato due genotipi di PRRSV: europeo (Tipo 1) e nordamericano (Tipo 2). Pur condividendo fenotipo clinico, genomica e periodo di comparsa, essi presentano una divergenza nucleotidica del 40% [2], suggerendo una prolungata evoluzione indipendente. L'orologio molecolare stima infatti che la separazione da un antenato comune (tramite un probabile salto di specie) sia avvenuta da decenni a oltre un secolo prima dell'esordio clinico [3].
Sebbene l'esatta origine e gli eventuali vettori restino tuttora ignoti, l'elevata frequenza di mutazione del virus e ricombinazione del genoma virale ha trasformato l'infezione in una pandemia persistente, caratterizzata dalla continua insorgenza di ceppi emergenti e riemergenti.

1.1.1 Classificazione e genoma

Appartenente all'ordine *Nidovirales* (famiglia *Arteriviridae*, assieme a *Coronaviridae* e *Roniviridae*), il PRRSV è un virus con envelope per il quale, a differenza di alcuni coronavirus, non è documentata trasmissione interspecifica [2]. Il suo genoma a RNA a singolo filamento positivo (+ssRNA), lungo 14,9-15,5 kb, comprende almeno 11 open reading frames (ORF). Attraverso due distinti meccanismi di trascrizione, queste ORF codificano diverse proteine accessorie, 16 proteine non strutturali (nsp) essenziali per la replicazione e 8 proteine strutturali necessarie per l'assemblaggio del virione.

Le regioni non tradotte (5' e 3' UTR) fiancheggiano il genoma e regolano replicazione e traduzione tramite strutture secondarie a RNA. Il 5' UTR (con Cap putativo di tipo 1) e il 3' UTR presentano un'elevata conservazione intragenotipo (~96%), ma una limitata omologia tra i Tipi 1 e 2 (rispettivamente ~50% e 70%). La porzione prossimale al 5' (~12 kb) ospita le ORF1a e ORF1b sovrapposte, tradotte direttamente dall'RNA genomico tramite *frameshift* ribosomiale. Le grandi poliproteine risultanti (pp1a, pp1a-nsp2N, pp1a-nsp2TF

e pp1ab) subiscono clivaggi co- e post-traduzionali da parte di quattro proteinasi virali (PLP1α, PLP1β, PLP2 e la serina-proteinasi principale) [2], generando le 16 proteine non strutturali (nsp1-nsp12) fondamentali per il complesso di replicazione.

Le proteine strutturali sono codificate dalle ORF al 3' (ORF2-7) ed espresse tramite RNA subgenomici (sgRNA2-7) derivati da un intermedio a filamento negativo. Pur essendo geneticamente policistronici, tali sgRNA agiscono come trascritti mono/bicistronici traducendo solo la ORF all'estremità 5'.
Il virione si articola in tre strutture: il complesso glicoproteico minore (GP2, GP3, GP4 dagli sgRNA 2-4), estensivamente N-glicosilato e vitale per l'ingresso cellulare; il complesso glicoproteico maggiore, un eterodimero legato da ponti disolfuro tra GP5 (sgRNA5) e proteina di membrana M (sgRNA6); e il nucleocapside, formato da omodimeri della proteina N (sgRNA7) per l'impacchettamento dell'RNA (unica proteina strutturale priva di domini transmembrana) [2]. Considerando anche la recente scoperta di isoforme di nsp2 incorporate nel virione [4], questa complessa architettura espone al sistema immunitario oltre dieci diverse proteine, evidenziando la profonda plasticità del PRRSV.

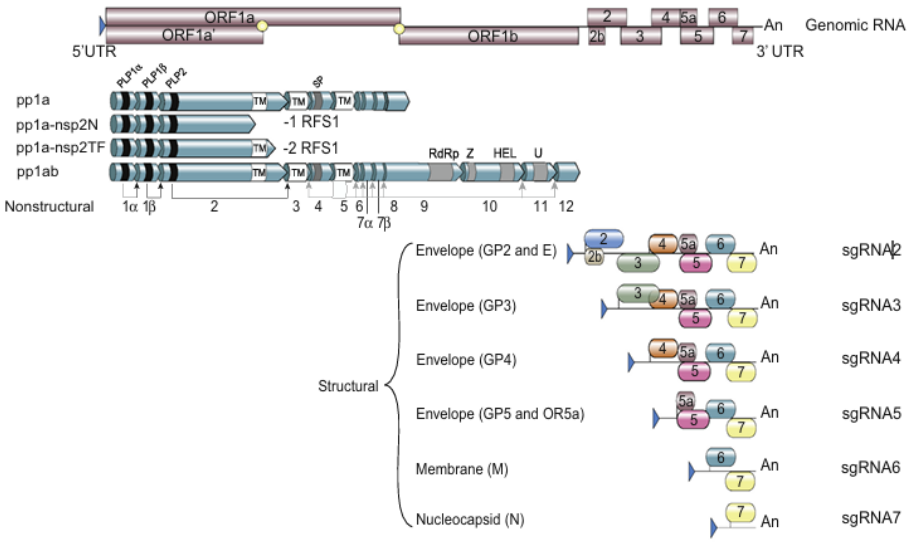


Figura 1: Genoma di PRRSV, trascrizione e traduzione [2]

1.1.2 Replicazione

Il ciclo replicativo del PRRSV associa il riarrangiamento delle membrane cellulari dell'ospite (per stabilire i complessi di replicazione virale) alla sintesi degli acidi nucleici. Dopo l'ingresso, l'RNA genomico positivo funge direttamente da mRNA per la sintesi della replicasi. Le subunità nsp2 e nsp3 (codificate dall'ORF1a) sfruttano i propri domini transmembrana per riarrangiare il reticolo endoplasmatico (ER), inducendo vescicole a doppia membrana (DMV) perinucleari che proteggono e ancorano i complessi replicativi. Il core enzimatico, derivato dall'ORF1b tramite *frameshift* ribosomiale, comprende l'RdRp (nsp9), l'elicasi (nsp10) e l'endoribonucleasi NendoU (nsp11). Poiché la RdRp

virale è priva di attività di *proofreading* in direzione 3' [2], la sintesi dell'RNA avviene con un altissimo tasso di errore, guidando la rapida evoluzione e l'estrema variabilità genetica dei ceppi di campo.

Mentre il gRNA intero viene sintetizzato per l'incapsidamento nei nuovi virioni, le proteine strutturali sono espresse tramite trascrizione discontinua [2]. Questo meccanismo genera un set annidato di RNA subgenomici (sgRNA) mediante il "salto" e la ricongiunzione del macchinario trascrizionale, una flessibilità che favorisce intrinsecamente frequenti eventi di ricombinazione genomica. L'efficienza dell'intero processo richiede l'interazione coordinata tra complessi elementi regolatori secondari (*cis-acting elements*), situati nelle estremità 5' e 3' UTR, e diverse proteine virali strutturali e non strutturali.

1.2 PS10 come composto antivirale

Il PS10 (2-[(2,4-diidrossifenil) sulfonil] isoindolina-4,6-diolo), noto inibitore della piruvato deidrogenasi chinasi (PDK) per la cardiomiopatia diabetica [5], è emerso da recenti screening come potente inibitore del PRRSV. Dotato di bassa citotossicità, abbatte l'infezione in modo dose-dipendente sia su linee permissive (Marc-145) sia sui bersagli primari (PAMs). La sua robusta attività ad ampio spettro su ceppi PRRSV-1 e PRRSV-2 supera le criticità legate all'elevata variabilità genetica che limita gli attuali vaccini vivi attenuati (MLV). A differenza dei MLV, che possono persistere, ricombinare con ceppi di campo e generare varianti virulente [6], l'uso di una piccola molecola come il PS10 azzera il rischio di ricombinazione e ripristino della virulenza. Infine, esprimendo la massima efficacia in pre-trattamento, il composto si profila come un eccellente agente profilattico per il controllo in allevamento.

Gli studi meccanicistici escludono un'azione virucida diretta sulla particella virale, confermando che il PS10 inibisce specificamente la replicazione intracellulare tramite un duplice meccanismo. Da un lato, agisce sull'ospite sopprimendo l'up-regolazione di HSP90 (chaperone essenziale per il PRRSV) indotta dall'infezione; questo blocca la diffusione del virus e mitiga l'immunopatologia attenuando le citochine pro-infiammatorie (IL-6, IL-8, TNF-α). Dall'altro, colpisce direttamente il macchinario replicativo virale: simulazioni di docking e saggi CETSA dimostrano infatti che il PS10 si lega fisicamente alle proteine nsp2, nsp3, nsp10 e nsp11, destabilizzandole e inducendone la degradazione selettiva.

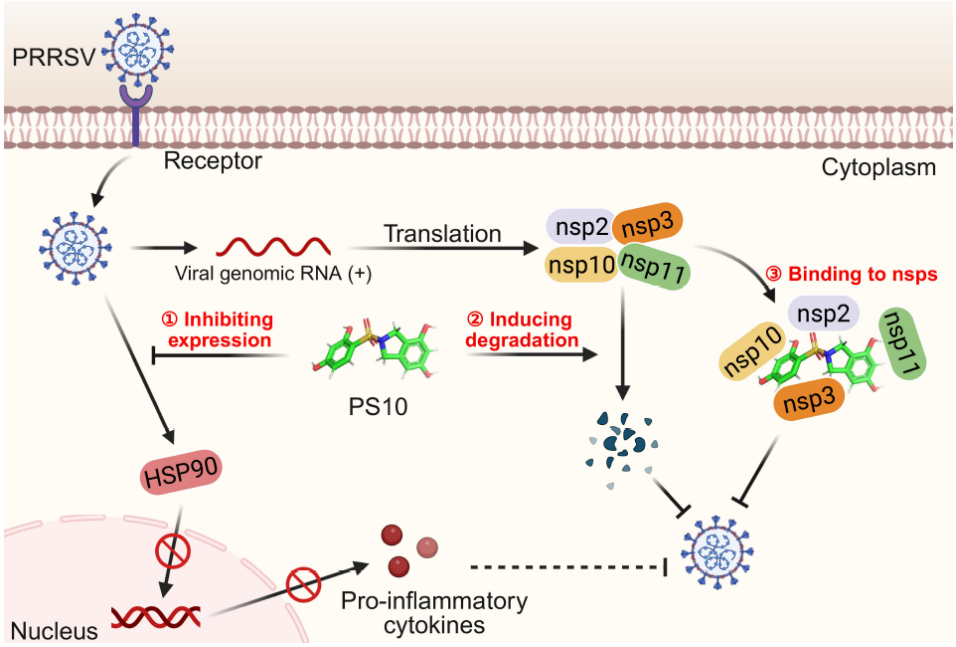


Figura 2: Modello schematico che illustra il meccanismo di inibizione della replicazione del PRRSV mediata da PS10

2 Approccio sperimentale: materiali e metodi

2.1 Cellule e virus

In questo studio sono state utilizzate quattro linee cellulari: HEK293T (cellule renali embrionali umane), Marc-145 (cellule epiteliali renali di scimmia) e cellule HeLa sono state coltivate in terreno DMEM (Dulbecco's modified Eagle's medium) integrato con il 10% di siero fetale bovino (FBS); i macrofagi alveolari suini primari (PAMs), che rappresentano le cellule bersaglio naturali per l'infezione da PRRSV, sono stati isolati da suinetti di 4 settimane negativi al PRRSV seguendo protocolli consolidati, per poi essere coltivati in terreno RPMI 1640 (Gibco) contenente il 10% di FBS.
Sono stati impiegati i ceppi PRRSV-2 JXA1, SD16, TA-12, WUH3, NADC30 e CH-1a, oltre al ceppo PRRSV-1 BJEU06-1. Tutti gli stock virali utilizzati sono stati propagati e titolati in cellule Marc-145.

2.2 Reagenti e anticorpi

I reagenti chimici e gli inibitori utilizzati comprendono la piccola molecola PS10, l'MG132, la clorochina (CQ), lo Z-VAD, la tanespimicina (17-AAG) e l'inibitore di NF-κB BAY 11-7082. Per le colture e i saggi cellulari si è fatto uso di TNF-α umano ricombinante, DAPI (1:1000) e polietilenimmina (PEI). Per quanto riguarda l'analisi proteica, sono stati utilizzati l'anticorpo monoclonale primario anti-N del PRRSV (1:3000) e gli anticorpi anti-GAPDH (1:5000), anti-tag mCherry (1:2000), nonché gli anticorpi diretti contro HSP90, HSP90AA1 e HSP90AB1 (tutti impiegati ad una diluizione 1:1000). Infine,

per la rilevazione sono stati adoperati anticorpi secondari anti-topo (1:10000) e anti-coniglio (1:10000) coniugati con HRP, insieme ad anticorpi di capra anti-topo coniugati con i fluorocromi Alexa Fluor 488 (1:1000) e Alexa Fluor 555 (1:1000).

2.3 Saggio di citotossicità

Per determinare gli effetti dei trattamenti sulla vitalità cellulare è stato impiegato il saggio colorimetrico CCK-8 (Cell Counting Kit-8). Le linee cellulari Marc-145 o PAMs sono state seminate in piastre da 96 pozzetti. A seguito dell'esposizione ai vari composti per un periodo di 24 ore, il terreno di coltura è stato supplementato con 10 μL/pozzetto di soluzione CCK-8. Dopo un'ulteriore incubazione di 1 ora, necessaria per lo sviluppo della reazione colorimetrica, i valori di assorbanza sono stati quantificati a 450 nm tramite l'utilizzo di uno spettrofotometro per micropiastre.

2.4 Estrazione di RNA e RT-qPCR

L'RNA totale è stato isolato dalle colture cellulari (Marc-145, HeLa o PAMs) impiegando il reagente TRIeasy, e successivamente retrotrascritto in cDNA avvalendosi del kit ABScript Neo RT Master Mix per qPCR con gDNA Remover. Le reazioni di amplificazione mediante Real-Time PCR sono state allestite utilizzando il BrightCycle Blue Universal SYBR Green qPCR Mix con UDG ed eseguite sul sistema termociclatore QuantStudio 3.
I livelli di espressione genica relativa sono stati calcolati applicando il metodo $2^{-\Delta\Delta CT}$. I dati sono stati normalizzati utilizzando come geni *housekeeping* di riferimento GAPDH per le linee cellulari Marc-145 e HeLa, e HPRT1 per i macrofagi alveolari suini (PAMs).

2.5 Western blotting

L'estrazione delle proteine totali è stata effettuata lisando le cellule in tampone RIPA supplementato con l'inibitore delle proteasi PMSF 1 mM, mantenendo i campioni in ghiaccio per 30 minuti. I lisati proteici sono stati separati mediante elettroforesi su gel di poliacrilammide in presenza di SDS (SDS-PAGE) e successivamente trasferiti su membrane in PVDF.
Per prevenire i legami aspecifici, le membrane sono state saturate per 2 ore a temperatura ambiente utilizzando una soluzione al 5% di latte scremato in polvere. È seguita l'incubazione con gli anticorpi primari specifici *overnight* a 4°C. Dopo tre lavaggi, le membrane sono state incubate per 1 ora a temperatura ambiente con i rispettivi anticorpi secondari coniugati con l'enzima perossidasi di rafano (HRP). Infine, i segnali proteici sono stati visualizzati impiegando un kit ECL per la rilevazione in chemiluminescenza amplificata.

2.6 Immunofluorescenza indiretta (IFA)

Le cellule sono state fissate impiegando una soluzione di paraformaldeide (PFA) al 4% per 15 minuti a temperatura ambiente. Successivamente, è stata indotta

la permeabilizzazione delle membrane cellulari mediante un trattamento di 5 minuti con Triton X-100 allo 0,5%.
A seguito di tre lavaggi in soluzione salina tamponata con fosfato (PBS), i siti di legame aspecifici sono stati saturati incubando i campioni con albumina di siero di bovino (BSA) all'1% per 1 ora a temperatura ambiente. Le cellule sono state quindi incubate *overnight* a 4°C con gli anticorpi primari specifici. Il giorno seguente, dopo ulteriori tre lavaggi in PBS, è stata condotta un'incubazione di 1 ora a temperatura ambiente con anticorpi secondari coniugati con fluorocromi. Per l'identificazione dei nuclei cellulari, i campioni sono stati controcolorati con DAPI per 5 minuti. Le immagini finali sono state acquisite avvalendosi di un microscopio a fluorescenza invertito (Nikon ECLIPSE Ti2).

2.7 Titolazione virale mediante saggio delle placche

Le cellule Marc-145, seminate in piastre da sei pozzetti, sono state infettate con diluizioni seriali 1:10 di PRRSV e incubate per 1 ora, prevedendo una blanda agitazione delle piastre ogni 15 minuti per favorire l'assorbimento virale. Terminato il periodo di infezione, l'inoculo è stato rimosso e i monostrati cellulari sono stati lavati con PBS. Successivamente, le cellule sono state ricoperte con un terreno semisolido costituito da DMEM addizionato con l'1% di agarosio a basso punto di fusione e il 2% di FBS.
A seguito della solidificazione dell'agarosio, le piastre sono state incubate a 37°C in un'atmosfera al 5% di CO_2 per 72 ore. Al termine dell'incubazione, previa rimozione dello strato di agarosio, le placche di lisi sono state visualizzate al microscopio ottico mediante colorazione con cristal violetto.

2.8 Interazione diretta PRRSV - PS10

Al fine di valutare l'interazione diretta con i virioni, il PRRSV è stato incubato con concentrazioni crescenti di PS10 per 2 ore a 37°C. Successivamente, i complessi virus-composto sono stati isolati mediante dispositivi di filtrazione centrifuga. A seguito di tre lavaggi con terreno basale, effettuati per rimuovere il composto PS10 non legato, i virioni purificati sono stati risospesi e inoculati su cellule Marc-145 per la successiva analisi dell'infettività a 24 ore dall'inoculo.

2.9 Trasfezione

I plasmidi codificanti le proteine non strutturali (nsp) del PRRSV sono stati impiegati per gli esperimenti di trasfezione. Le cellule HEK-293T sono state seminate in piastre da 12 pozzetti e, al raggiungimento di una confluenza cellulare pari a circa l'80%, sono state trasfettate con i suddetti plasmidi utilizzando la polietilenimmina (PEI) come agente trasfettante.
Sei ore post-trasfezione, le colture cellulari sono state trattate in presenza o in assenza del composto PS10. Infine, a 24 ore dall'avvenuta trasfezione, i campioni cellulari sono stati raccolti per la successiva analisi dell'espressione proteica mediante Western blot.

2.10 Cellular Thermal Shift Assay (CETSA)

Le cellule HEK293, a 24 ore dalla trasfezione con i rispettivi plasmidi, sono state lisate utilizzando un tampone di lisi NP-40. Aliquote da 50 μL di lisato sono state incubate in presenza o in assenza del composto PS10 (40 μM) a 37°C per 30 minuti. I campioni sono stati successivamente suddivisi in frazioni e riscaldati per 3 minuti a diverse temperature (45°C, 50°C, 55°C, 60°C, 65°C e 70°C). A questo passaggio sono seguiti tre cicli di congelamento in azoto liquido e scongelamento a 25°C.
Dopo una centrifugazione a 12.000 $\times$ g per 20 minuti a 4°C, i surnatanti sono stati trasferiti in nuove provette, miscelati con il tampone di caricamento, denaturati mediante ebollizione a 100°C per 10 minuti e, infine, analizzati tramite Western blot.

2.11 Docking molecolare

Al fine di indagare le interazioni proteina-piccola molecola, sono state condotte analisi di docking molecolare. Le strutture dei ligandi sono state acquisite dal database PubChem, mentre i modelli strutturali delle proteine sono stati predetti avvalendosi del server AlphaFold 3. Le simulazioni di docking sono state infine eseguite utilizzando la piattaforma web CB-Dock2.

2.12 Analisi statistica

I dati ottenuti sono stati analizzati utilizzando il software GraphPad Prism 8. I confronti a coppie sono stati eseguiti mediante il test t di Student, mentre per i confronti tra gruppi multipli è stata applicata l'analisi della varianza (ANOVA) a una o a due vie. La soglia di significatività statistica è stata fissata per un valore di $P < 0.05$, con i livelli di significatività denotati come $*P < 0{,}05$, $**P < 0{,}01$ e $***P < 0{,}001$. Le differenze non significative sono contrassegnate come "ns".

3 Risultati e discussione

3.1 PS10 inibisce la replicazione di PRRSV in cellule epiteliali renali di scimmia (Marc-145) e in macrofagi alveolari suini (PAMs)

Al fine di identificare specifici inibitori del PRRSV tramite screening di piccole molecole, monostrati di cellule Marc-145 sono stati pre-incubati per 2 ore con vari composti (alla concentrazione di 10 μM) ed esposti successivamente ad un ceppo di PRRSV esprimente la luciferasi, impiegando una molteplicità di infezione (MOI) pari a 0.5. A 24 ore dall'infezione, la molecola PS10 ha indotto una drastica riduzione dell'attività luciferasica (Gluc), dimostrando una forte efficacia antivirale (Figura 3). Tali risultati non sono attribuibili a citotossicità aspecifica: il test di vitalità CCK-8 ha infatti escluso effetti tossici per concentrazioni di PS10 fino a 40 μM (Figura 4).

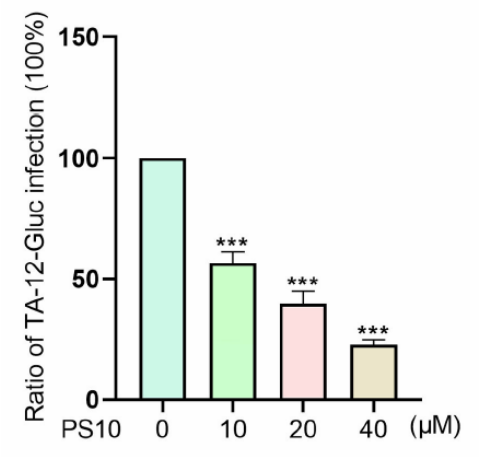


Figura 3: Quantificazione dell'attività luciferasica (Gluc) in cellule Marc-145 a 24 ore dall'infezione

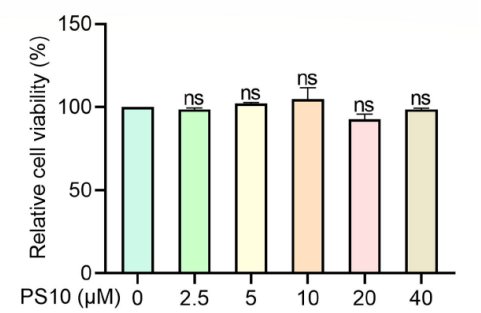


Figura 4: Vitalità cellulare di cellule Marc-145 saggiata mediante test CCK-8

Valutando l'efficacia sul ceppo PRRSV CH-1a, PS10 ha indotto una riduzione dose-dipendente dell'mRNA del gene N virale (Figura 5). Poiché i primer iniziali non discriminavano tra RNA genomico (gRNA) e mRNA subgenomici (sgmRNA), saggi di amplificazione specifici hanno confermato che la molecola sopprime entrambe le specie, compromettendo sia la replicazione che la trascrizione del genoma virale (Figura 6). Parallelamente, si è osservato un calo dose-dipendente della proteina N e dei titoli virali.
L'analisi cinetica ha infine evidenziato un'azione prolungata: PS10 ha soppresso stabilmente l'espressione di mRNA e proteina N, oltre alla produzione di progenie infettante (quantificata tramite saggio delle placche), in tutti i punti temporali analizzati (Figura 7).

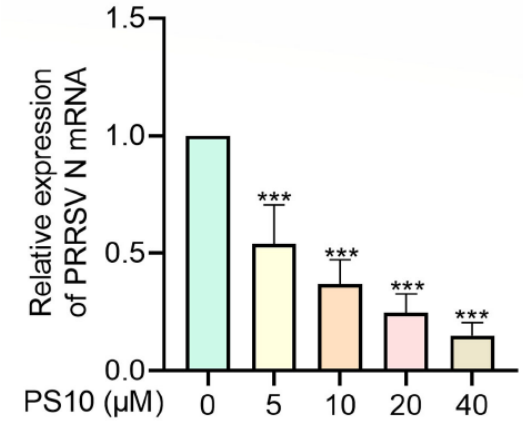


Figura 5: Quantificazione tramite RT-qPCR del livello di mRNA del gene virale N in cellule Marc-145

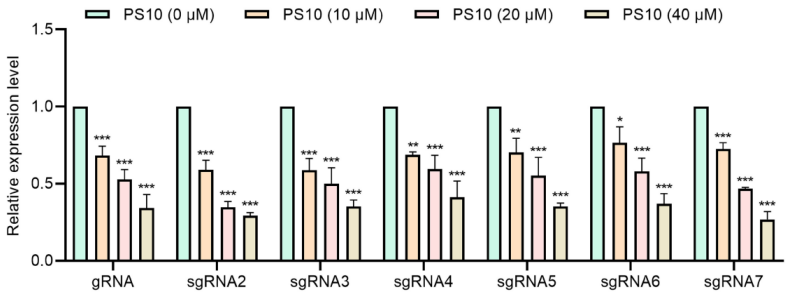


Figura 6: Quantificazione tramite RT-qPCR dei livelli di gRNA e sgRNA virali in cellule Marc-145

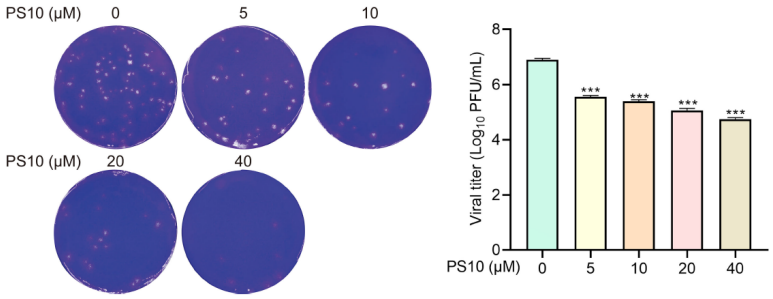


Figura 7: Saggio delle placche e titolo virale in cellule Marc-145

L'efficacia inibitoria di PS10 è stata testata anche sui macrofagi alveolari suini (PAMs), bersagli primari dell'infezione naturale da PRRSV. Saggi preliminari hanno escluso effetti citotossici su queste cellule per concentrazioni fino a 40 μM (Figura 8). Infettando le colture primarie con il ceppo PRRSV JXA1, il PS10 ha ridotto in modo dose-dipendente l'mRNA virale (Figura 9), l'abbondanza della proteina N (Figura 10) e la produzione di progenie virale (Figura 11), confermando una potente azione antivirale anche nei PAMs.

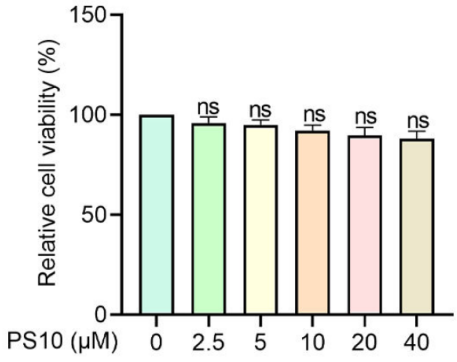


Figura 8: Vitalità cellulare di cellule PAMs saggiata mediante test CCK-8

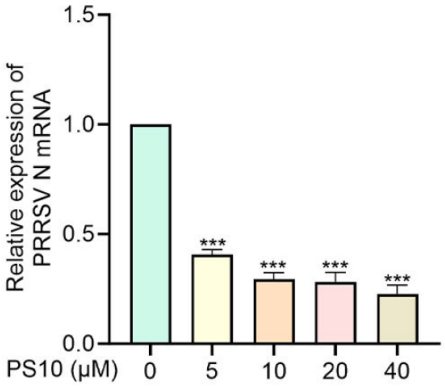


Figura 9: Quantificazione tramite RT-qPCR del livello di mRNA del gene virale N in cellule PAMs

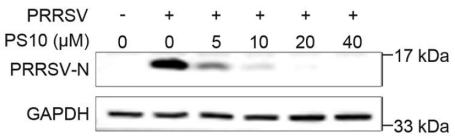


Figura 10: Quantificazione del livello della proteina virale N in cellule PAMs tramite Western Blotting

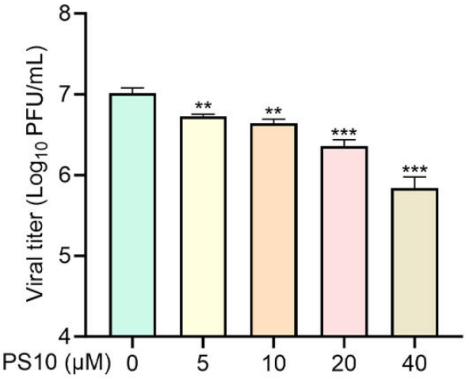


Figura 11: Titolo virale determinato mediante saggio delle placche in cellule PAMs

3.2 Attività anti-PRRSV di PS10 in condizioni di diversi regimi di trattamento

La finestra terapeutica del PS10 è stata delineata tramite saggi *time-of-addition* (Figura 12) articolati in tre fasi: pre-trattamento (2 ore prima dell'infezione), co-trattamento (in concomitanza con l'inoculo virale) e post-trattamento (2 ore dopo l'infezione). Sebbene tutti gli approcci abbiano inibito efficacemente mRNA (Figura 14), proteina N (Figura 13), titoli virali (Figura 15) e la relativa fluorescenza della proteina N (Figura 16), si è osservato un preciso gradiente di attività inibitoria. Il pre-trattamento è infatti risultato il protocollo più drastico nel bloccare la replicazione virale, risultando superiore sia al co-trattamento che al post-trattamento.

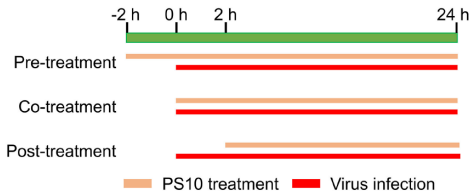


Figura 12: Diagramma schematico dei tre protocolli operativi

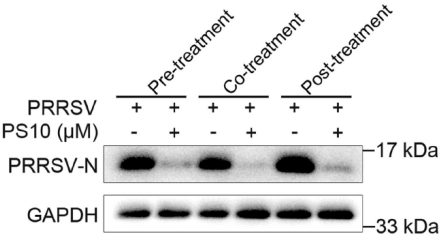


Figura 13: Quantificazione del livello della proteina virale N tramite Western Blotting nei tre regimi di trattamento

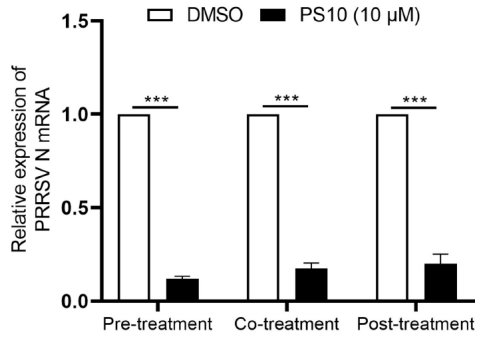


Figura 14: Quantificazione tramite RT-qPCR del livello di mRNA del gene virale N nei tre regimi di trattamento

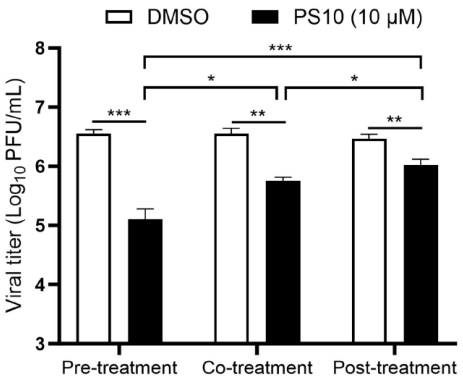


Figura 15: Titolo virale nei tre regimi di trattamento

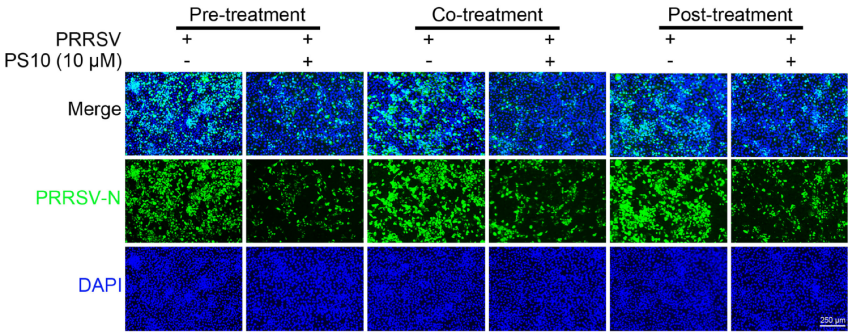


Figura 16: Intensità di fluorescenza della proteina virale N analizzata tramite IFA

3.3 PS10 non stabilisce una interazione diretta con la particella virale

Per escludere un'azione virucida diretta, sospensioni di PRRSV sono state co-incubate con diverse concentrazioni di PS10 (2 ore a 37°C). Dopo aver rimosso il composto non legato tramite ultrafiltrazione, i virioni sono stati impiegati per infettare cellule Marc-145. A 24 ore post-infezione (hpi), le analisi dell'mRNA (Figura 17), della proteina N (Figura 18) e dei titoli virali (Figura 19), non hanno mostrato riduzioni dell'infettività rispetto ai controlli. Ciò dimostra che il PS10 non inattiva o destabilizza direttamente il virione, ma agisce in una fase post-ingresso, colpendo bersagli replicativi virali o dell'ospite.

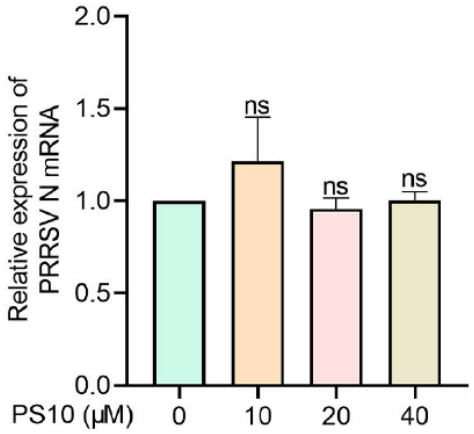


Figura 17: Quantificazione tramite RT-qPCR del livello di mRNA del gene virale N

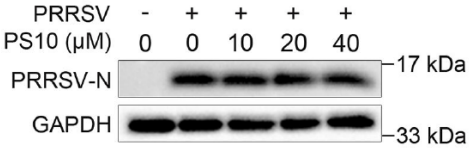


Figura 18: Quantificazione del livello della proteina virale N tramite Western Blotting

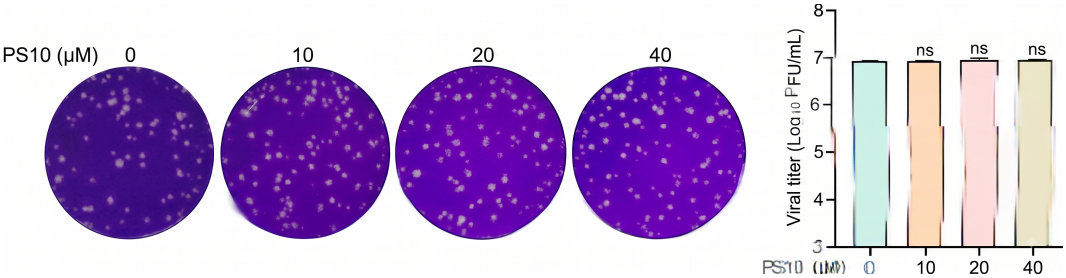


Figura 19: Saggio delle placche e titolo virale

3.4 Attività anti-PRRSV di PS10 nei confronti di diversi ceppi virali

Data l'alta variabilità genetica del PRRSV che compromette l'efficacia dei vaccini attuali [6] è stata indagata l'attività ad ampio spettro del PS10 su un pannello eterogeneo di isolati. L'esposizione dose-dipendente al composto ha abbattuto i livelli della proteina N e il relativo segnale di fluorescenza (Figura 20) in molteplici ceppi di PRRSV-2 (JXA1, SD16, TA-12, WUH3, NADC30). Questa forte efficacia inibitoria è stata confermata anche contro il genotipo 1 (PRRSV-1, ceppo BJEU06-1). Tali evidenze dimostrano che il PS10 possiede una robusta attività antivirale ad ampio spettro, in grado di contrastare efficacemente la diversità genetica del patogeno.

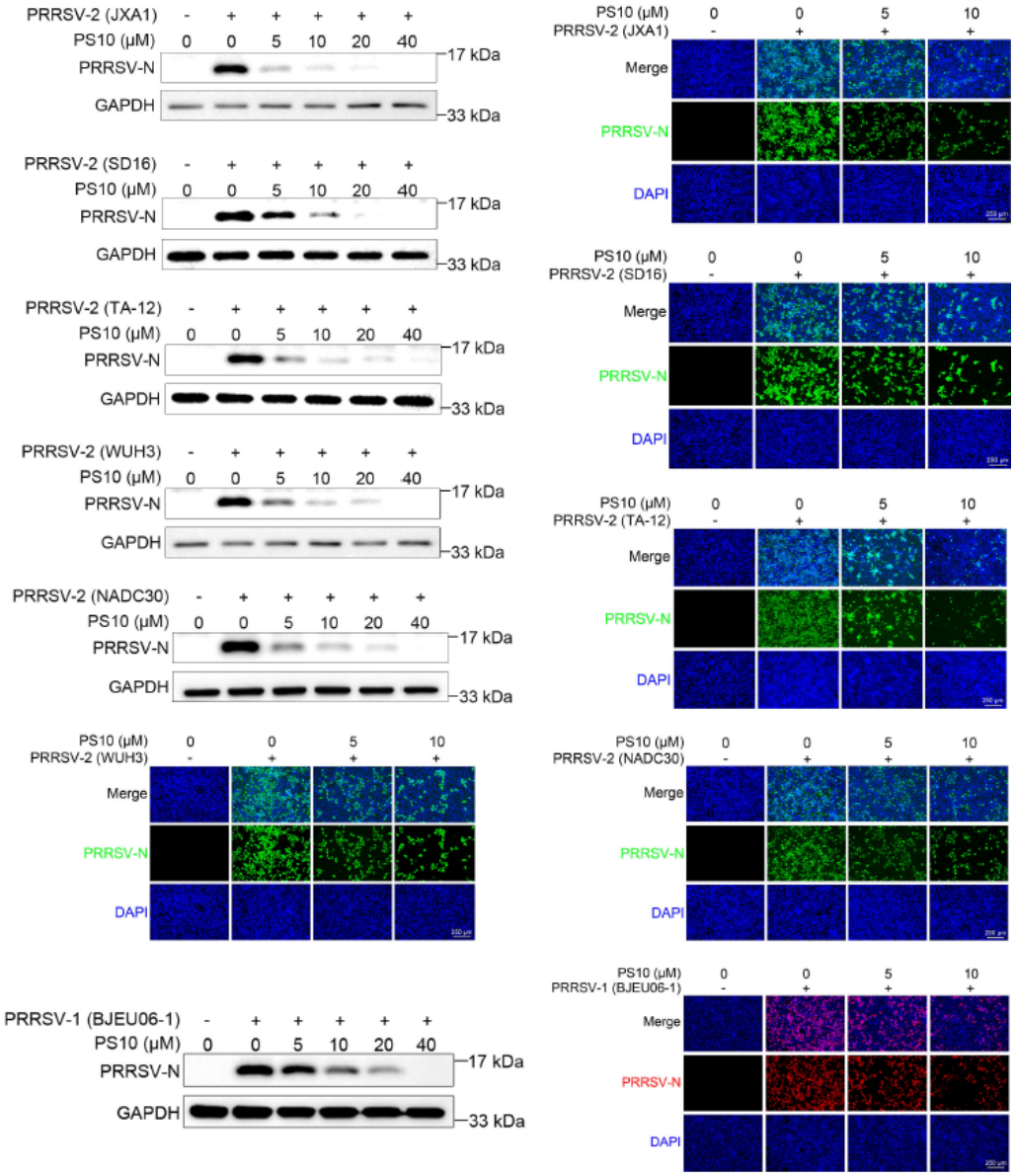


Figura 20: Quantificazione del livello della proteina virale N tramite Western Blotting per ogni ceppo virale saggiato e relativa visualizzazione tramite IFA

3.5 Inibizione specifica di PS10 a livello della fase di replicazione virale

Per definire il meccanismo d'azione del PS10, il composto è stato valutato nelle quattro fasi del ciclo vitale del PRRSV (adsorbimento, internalizzazione, replicazione e rilascio di progenie virale). La quantificazione dell'mRNA per l'antigene N ha escluso qualsiasi interferenza del farmaco con le fasi precoci di attacco recettoriale ed endocitosi (Figura 21). Analogamente, l'analisi dei titoli virali non ha evidenziato inibizioni sugli eventi tardivi di esocitosi e diffusione (Figura 22). Al contrario, la quantificazione dell'RNA ha dimostrato che il PS10 inibisce in modo drastico e specifico la sola fase di replicazione del PRRSV.

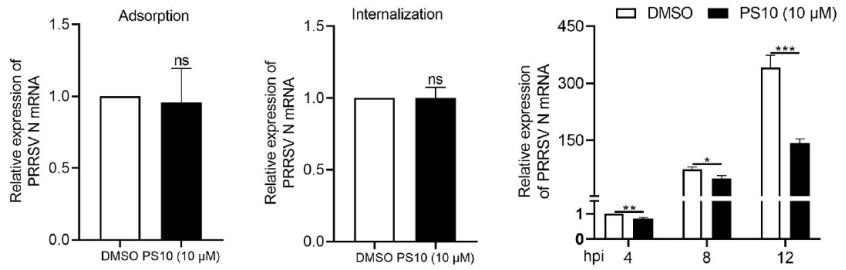


Figura 21: Quantificazione tramite RT-qPCR del livello di mRNA del gene virale N nelle fasi di adsorbimento (sx), internalizzazione (centro) e replicazione (dx)

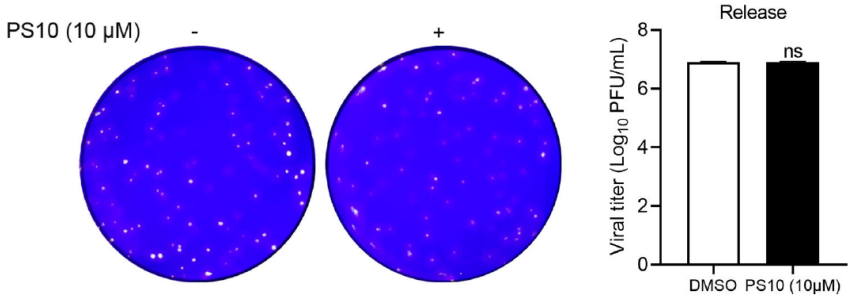


Figura 22: Quantificazione tramite RT-qPCR del livello di mRNA del gene virale N e saggio delle placche nella fase di rilascio

3.6 PS10 riduce la produzione di citochine pro-infiammatorie mediante down-regolazione dell'espressione di HSP90

È noto che il PS10 si leghi direttamente allo chaperone HSP90 [7], indispensabile per la replicazione del PRRSV. Valutando i livelli di questa proteina cellulare, si è prima osservato che l'infezione virale innesca una severa stimolazione (mRNA e accumulo proteico) dell'HSP90 totale e delle isoforme HSP90AA1 e HSP90AB1 (Figura 23). L'intervento farmacologico si è rivelato efficace nel bloccare questo processo: il trattamento con PS10 annulla significativamente l'aumento dei trascritti di HSP90AA1, HSP90AB1 e dell'HSP90 totale originariamente indotto dal virus (Figura 24).

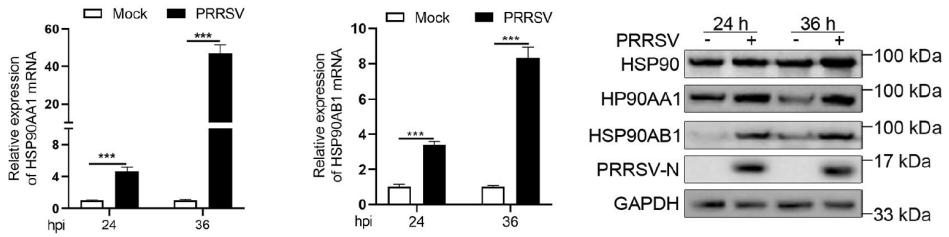


Figura 23: Quantificazione del livello degli mRNA di HSP90AA1 e HSP90AB1 post-infezione con PRRSV tramite RT-qPCR e delle proteine associate tramite Western Blotting

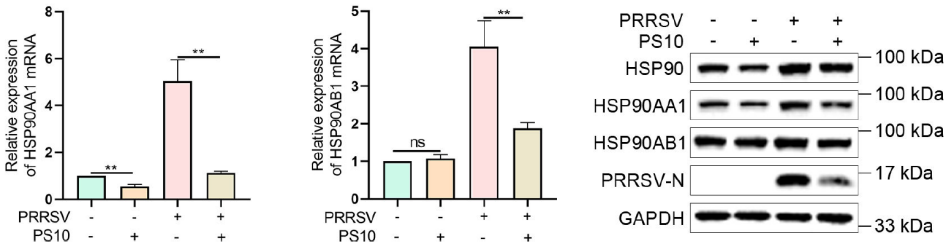


Figura 24: Quantificazione del livello degli mRNA di HSP90AA1 e HSP90AB1 post-infezione con PRRSV e trattamento con PS10 tramite RT-qPCR e delle proteine associate tramite Western Blotting

Per verificare se l'azione anti-PRRSV del PS10 sia mediata dalla modulazione dell'HSP90, è stato utilizzato il 17-AAG come inibitore di riferimento. Sulle cellule Marc-145 (dosi<10 μM, Figura 25), il 17-AAG abbatte in maniera dose-dipendente le copie genomiche (Figura 26), la proteina N e l'espressione di HSP90 totale e delle isoforme AA1/AB1 (Figura 27). Confrontando le due molecole, è emerso che la loro co-somministrazione genera un forte effetto additivo: pur preservando la vitalità cellulare (Figura 28), l'approccio combinato determina la massima soppressione di HSP90, HSP90AA1 e HSP90AB1 (Figura 30) e, di conseguenza, la più potente inibizione della replicazione virale.

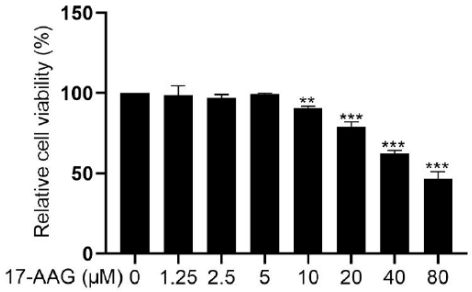


Figura 25: Vitalità cellulare post-trattamento con 17-AAG saggiata mediante test CCK-8

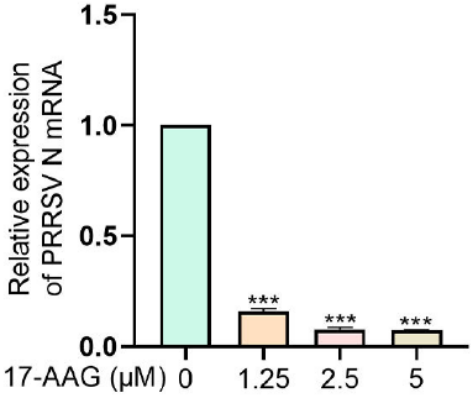


Figura 26: Quantificazione tramite RT-qPCR del livello di mRNA del gene virale N post-trattamento con 17-AAG

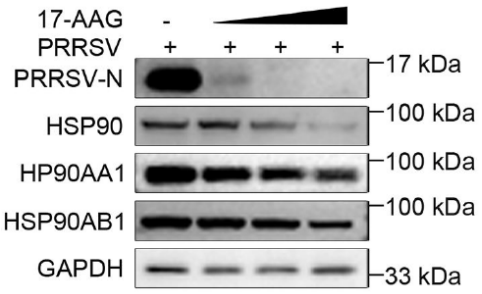


Figura 27: Quantificazione tramite Western Blotting dei livelli di proteina N, HSP90, HSP90AA1 e HSP90AB1 post-trattamento con 17-AAG

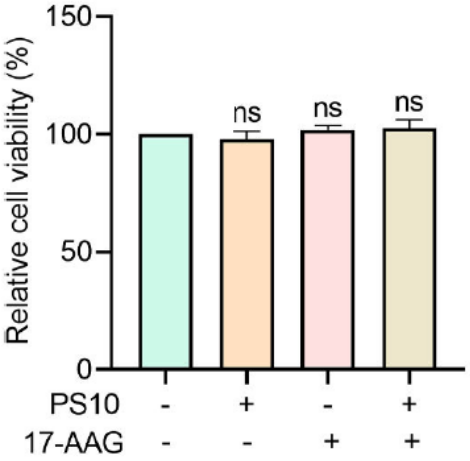


Figura 28: Vitalità cellulare dopo co-trattamento con 17-AAG e PS10 saggiata mediante test CKK-8

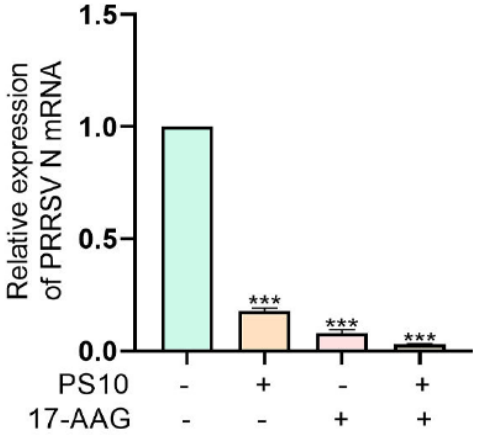


Figura 29: Quantificazione tramite RT-qPCR del livello di mRNA del gene virale N dopo co-trattamento con 17-AAG e PS10

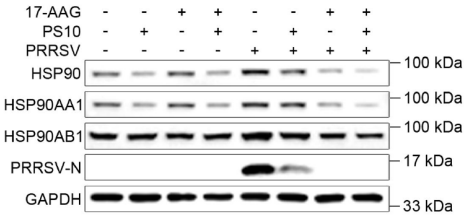


Figura 30: Quantificazione tramite Western Blotting dei livelli di proteina N, HSP90, HSP90AA1 e HSP90AB1 dopo co-trattamento con 17-AAG e PS10

Considerando il ruolo dell'HSP90 nell'infiammazione [8] e la "tempesta citochinica" indotta dal PRRSV, è stata indagata l'azione antinfiammatoria del PS10. Il trattamento abbatte in modo dose-dipendente l'espressione di IL-6, IL-8 e TNF-α innescata dal virus (Figura 31), effetto che risulta drasticamente potenziato dalla co-somministrazione con 17-AAG (Figura 32). Testando le molecole su cellule HeLa non infettate, ma stimolate con TNF-α esogeno, si è osservata un'analoga repressione citochinica (Figura 33).
Queste evidenze certificano che l'abbattimento dell'infiammazione da parte del PS10 è un meccanismo intrinseco legato all'inibizione dell'HSP90, e non un mero effetto secondario della ridotta replicazione virale.

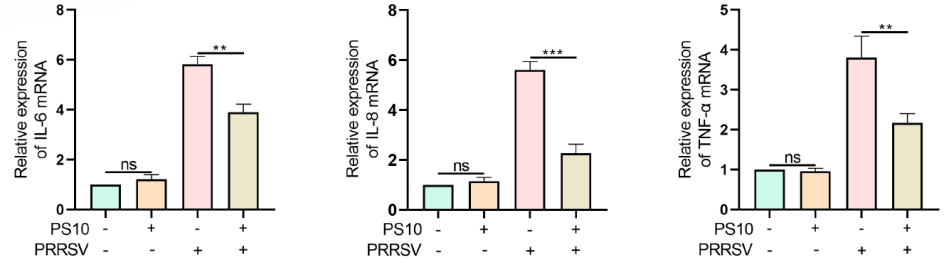


Figura 31: Quantificazione tramite RT-qPCR degli mRNA di IL-6, IL-8 e TNF-α post-trattamento con PS10

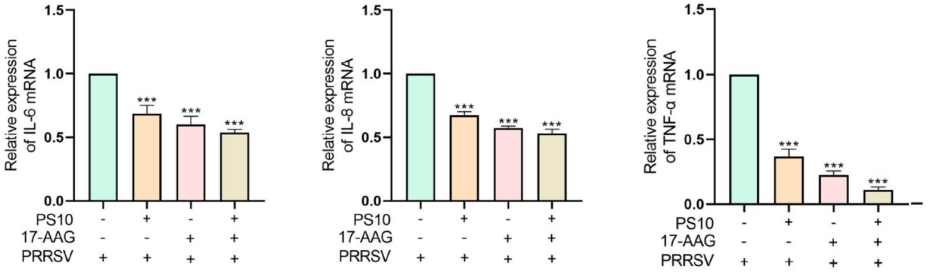


Figura 32: Quantificazione tramite RT-qPCR degli mRNA di IL-6, IL-8 e TNF-α dopo co-trattamento con 17-AAG e PS10

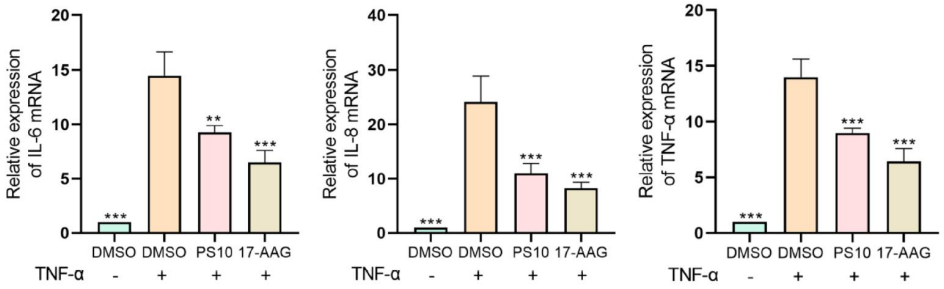


Figura 33: Quantificazione tramite RT-qPCR degli mRNA di IL-6, IL-8 e TNF-α su cellule HeLa non infettate

Per confermare l'interconnessione tra infiammazione e replicazione virale, l'uso dell'inibitore di NF-κB BAY 11-7082 ha evidenziato un calo dose-dipendente della proteina N (Figura 34). Questo risultato dimostra che la down-regolazione di HSP90 mediata dal PS10 abbatte la sintesi citochinica, innescando una forte azione immunomodulatoria che lavora in perfetta sinergia con i meccanismi antivirali per sopprimere drasticamente l'infezione.

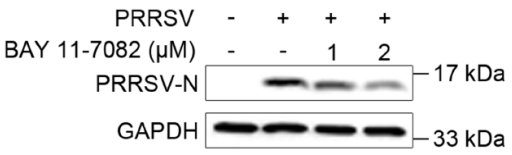


Figura 34: Quantificazione tramite Western Blotting della proteina N post-trattamento con BAY 11-7082

3.7 PS10 riduce l'espressione delle proteine virali nsp2, nsp3, nsp10 e nsp11

Poiché il PS10 colpisce la fase replicativa del PRRSV, ne è stato valutato l'impatto sulle proteine non strutturali (nsp). Su cellule HEK293T (la cui vitalità è risultata totalmente preservata fino a 40 μM, Figura 35), l'esposizione al composto ha innescato una significativa riduzione dose-dipendente dei livelli proteici di nsp2, nsp3, nsp10 e nsp11. Tale repressione risulta altamente selettiva, in quanto l'espressione di tutte le altre subunità nsp non ha subito alcuna alterazione (Figura 36).

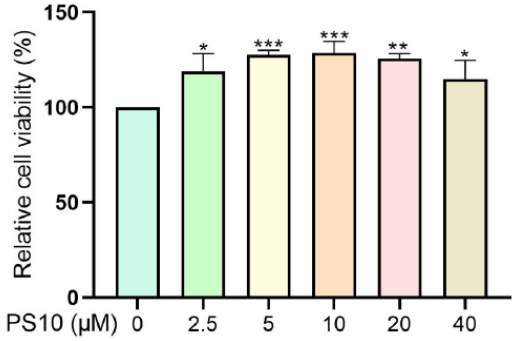


Figura 35: Vitalità cellulare saggiata mediante test CKK-8

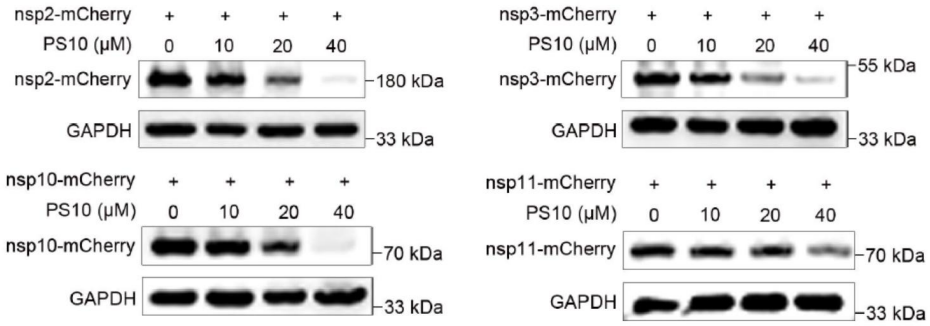


Figura 36: Quantificazione tramite Western Blotting di nsp2, nsp3, nsp10 e nsp11 a concentrazioni crescenti di PS10

Per verificare se il degrado delle nsp mediato dal PS10 dipendesse dai pathway catabolici cellulari, sono stati impiegati tre inibitori: CQ per l'autofagia, MG132 per il sistema ubiquitina-proteasoma e Z-VAD per l'apoptosi caspasi-dipendente. Nessuno di essi ha bloccato il calo di nsp2 indotto dal composto, mentre tutti hanno garantito un recupero parziale di nsp3, nsp10 e nsp11 (Figura 37). L'efficacia del PS10 su nsp2 e nsp10 è stata confermata anche durante l'infezione attiva.
Il recupero di nsp10 tramite Z-VAD è coerente con il suo ruolo di induttore apoptotico (via caspasi-8) nelle infezioni avanzate [9]. Il parziale recupero di nsp3 con CQ si allinea al ruolo di questa proteina nel blocco virale della fusione autofagosoma-lisosoma. Al contrario, il mancato ripristino di nsp2 da parte

della CQ suggerisce che il suo degrado indotto da PS10 si verifichi a monte o eludendo il blocco lisosomiale, nonostante la nsp2 interagisca normalmente con marcatori autofagici (es. LC3) per favorire la replicazione virale [9].

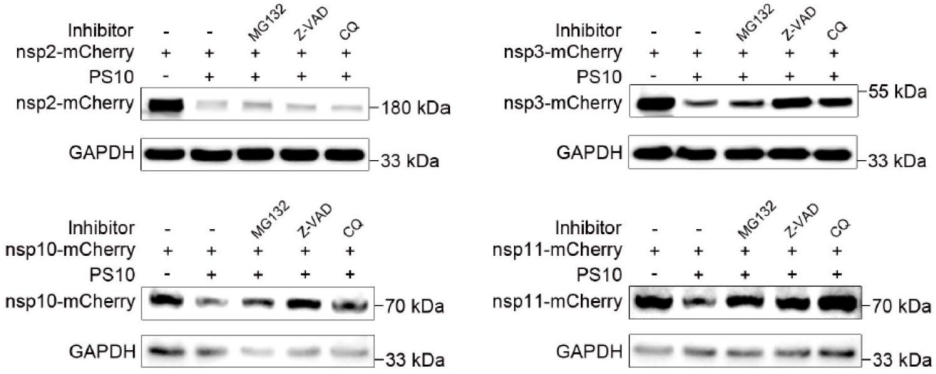


Figura 37: Quantificazione tramite Western Blotting dei livelli di nsp2, nsp3, nsp10 e nsp11 in presenza di CQ, MG132 e Z-VAD

Dato che il PS10 destabilizza irreversibilmente nsp2 e nsp3 (fondamentali per il complesso di replicazione-trascrizione, RTC), si è indagato il suo impatto diretto sulla replicazione virale quantificando l'RNA a doppio filamento (dsRNA). Coerentemente con l'ipotesi di partenza, il trattamento ha inibito in modo drastico la sintesi di questo intermedio replicativo obbligato del PRRSV (Figura 38).

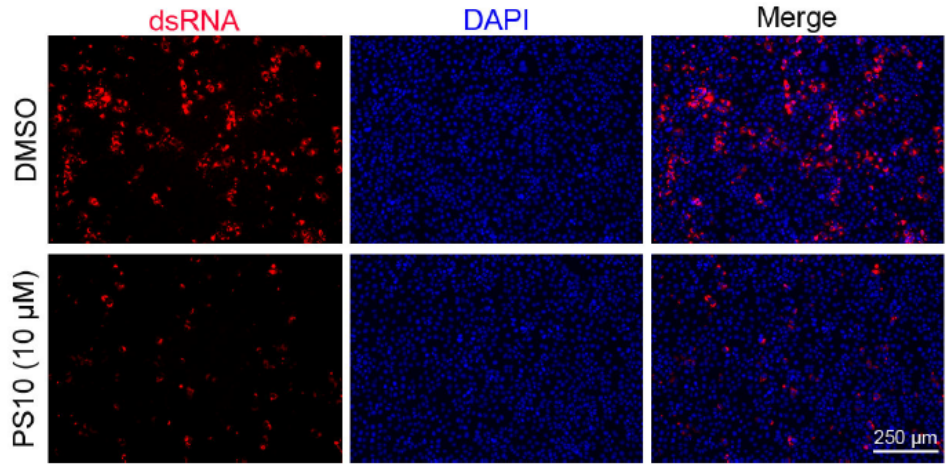


Figura 38: Rilevazione del dsRNA post-trattamento con PS10 tramite IFA

3.8 Interazione tra PS10 e le proteine virali nsp1, nsp3, nsp10 e nsp11

Per verificare se il PS10 interagisse direttamente con nsp2, nsp3, nsp10 e nsp11, analisi iniziali di docking molecolare hanno confermato la formazione di complessi termodinamicamente favorevoli. Tali dati sono stati validati *in vitro* tramite saggio di stabilità termica cellulare (CETSA) su estratti di HEK293T

esprimenti le nsp. Sotto stress termico, l'esposizione a PS10 (40 μM, vs veicolo DMSO) ha incrementato drasticamente la stabilità delle quattro proteine ritardandone la degradazione (Figura 39).
L'integrazione di queste evidenze prova in modo conclusivo il legame fisico diretto tra il composto PS10 e le proteine virali nsp2, nsp3, nsp10 e nsp11.

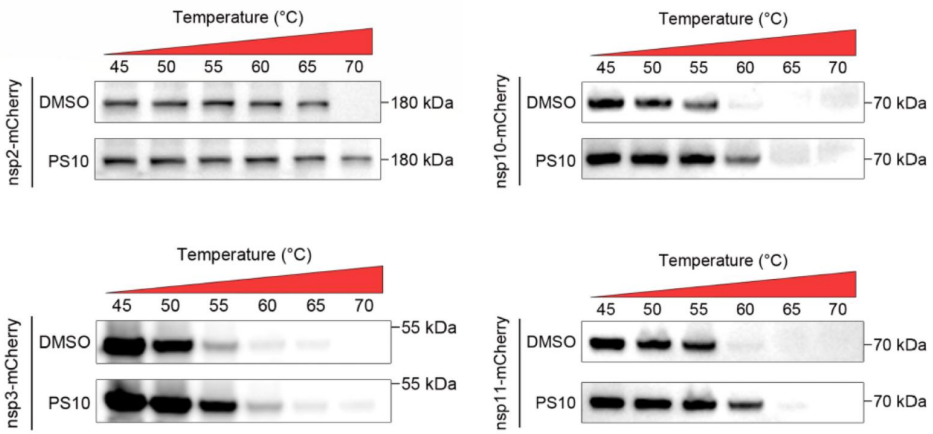


Figura 39: Cellular Thermal Shift Assay (CETSA)

4 Considerazioni e conclusione

La minaccia del PRRSV per la zootecnia è esacerbata dall'estrema variabilità genetica e dalle frequenti ricombinazioni che vanificano i vaccini attuali [6], rendendo cruciale lo sviluppo di nuovi farmaci. Oltre a composti già noti come fangchinolina e cefarantina (target CD163) [10], iperoside (modulatore di TLR4/NF-κB e p62-Nrf2-Keap1) [11], matrina e acido glicirrizico [12], un recente screening ha identificato il PS10. Questo inibitore unisce bassi costi di sintesi ad una potente attività antivirale *in vitro* e alta tollerabilità su cellule Marc-145 e macrofagi alveolari suini (PAMs). Sebbene nei PAMs l'efficacia sia lievemente ridotta (probabilmente per differenze cellulari e di ceppo virale) e si noti un'eterogeneità nelle placche di lisi, il PS10 rimane un eccellente candidato terapeutico. Infine, il sequenziamento ha rivelato una mutazione virale indotta dal PS10 (dati non mostrati), che potrebbe comportare un'attenuazione della fitness o l'insorgenza di resistenza.

I saggi di somministrazione indicano che l'efficacia del PS10 è massima in pre-trattamento e cala nelle fasi tardive, suggerendone un impiego d'elezione come profilassi.
Pur privo di azione virucida diretta sui virioni, il composto garantisce una potente inibizione ad ampio spettro capace di superare l'elevata plasticità genetica del PRRSV.
A livello meccanicistico, il PS10 blocca selettivamente la replicazione prendendo di mira lo chaperone dell'ospite HSP90: sopprimendo la sua iper-espressione indotta dal virus, la molecola priva il macchinario replicativo di un fattore essenziale per la stabilizzazione delle proteine virali. Questa dinamica inibitoria

è coerente con il noto ruolo provirale dell'HSP90 già accertato per altri patogeni come ASFV, HSV-1 e BTV.

Durante l'infezione, il PRRSV attiva NF-κB per up-regolare le citochine proinfiammatorie. In tale processo l'HSP90 è cruciale, poiché stabilizza IKK-β (mantenendo attivo NF-κB) e facilita l'attivazione dell'inflammasoma NLRP3. I dati confermano che il PS10, analogamente all'inibitore canonico 17-AAG, mitiga drasticamente questa tempesta citochinica reprimendo l'HSP90. Testando le due molecole su cellule non infettate ma stimolate con TNF-α esogeno, entrambe hanno depresso la risposta citochinica: ciò certifica che l'azione antinfiammatoria del PS10 è un meccanismo intrinseco mediato dalla down-regolazione di HSP90, e non un mero effetto secondario del calo della carica virale. Tale dinamica suggerisce la potenziale efficacia del composto anche contro altri patogeni che sfruttano il medesimo asse.

Indagando l'azione del PS10 sulla replicazione del PRRSV, si è osservata una drastica riduzione intracellulare di specifiche proteine non strutturali. Mentre l'impiego degli inibitori CQ, MG132 o Z-VAD ha garantito un parziale ripristino di nsp3, nsp10 e nsp11, la deplezione di nsp2 è risultata totalmente refrattaria, suggerendo un meccanismo degradativo distinto (con soppressione di nsp2 e nsp10 confermata anche in infezione attiva). Tali proteine sono vitali per il patogeno: nsp2 agisce da proteasi PLP2, nsp3 è un elemento transmembrana del complesso di replicazione-trascrizione, nsp10 funge da elicasi e nsp11 da endoribonucleasi [2].
Saggi CETSA e docking molecolare hanno infine accertato un legame fisico diretto tra il PS10 e queste subunità, interazione sterica che giustifica la soppressione della loro espressione.

È stato inoltre osservato che l'esposizione al PS10 incrementa sensibilmente la vitalità cellulare nei monostrati HEK-293T, mantenendo invece un profilo neutrale su Marc-145 e PAM. Questo specifico effetto pro-sopravvivenza suggerisce una dipendenza dalle differenze nel metabolismo basale o nell'omeostasi dello stress tra le diverse linee cellulari, ponendo le basi per future indagini mirate.

In conclusione, questo studio dimostra per la prima volta l'efficacia del PS10 contro il PRRSV attraverso un duplice meccanismo d'azione. Da un lato, la molecola down-regola l'espressione di HSP90, inibendo così la proliferazione virale e mitigando l'infiammazione; dall'altro, instaura un legame fisico diretto con nsp2, nsp3, nsp10 e nsp11, inducendone la degradazione mirata. Tali evidenze elevano il PS10 a promettente molecola *lead* per nuove terapie anti-PRRSV, suggerendone inoltre un impiego come antivirale ad ampio spettro grazie alla capacità di colpire simultaneamente fattori patogeni e bersagli dell'ospite.

5 Bibliografia

[1] Yongjie Chen et al. «Small-Molecule PS10 Inhibits PRRSV Replication by Targeting HSP90 and Multiple Viral Non-Structural Proteins». In: *Journal of Virology* 100 (Mar. 24, 2026), e02121–25. ISSN: 0022-538X, 1098-5514. DOI: 10.1128/jvi.02121-25.

[2] Matthew A. Kappes and Kay S. Faaberg. «PRRSV Structure, Replication and Recombination: Origin of Phenotype and Genotype Diversity». In: *Virology* 479–480 (May 2015), pp. 475–486. ISSN: 00426822. DOI: 10.1016/j.virol.2015.02.012.

[3] Sook Hee Yoon et al. «Complete Genome Sequences of Porcine Reproductive and Respiratory Syndrome Viruses: Perspectives on Their Temporal and Spatial Dynamics». In: *Molecular Biology Reports* 40 (Oct. 2013), pp. 6843–6853. ISSN: 0301-4851. DOI: 10.1007/s11033-013-2802-1.

[4] Matthew A. Kappes, Cathy L. Miller, and Kay S. Faaberg. «Porcine Reproductive and Respiratory Syndrome Virus Nonstructural Protein 2 (Nsp2) Topology and Selective Isoform Integration in Artificial Membranes». In: *Virology* 481 (July 2015), pp. 51–62. ISSN: 00426822. DOI: 10.1016/j.virol.2015.01.028.

[5] Cheng-Yang Wu et al. «A Novel Inhibitor of Pyruvate Dehydrogenase Kinase Stimulates Myocardial Carbohydrate Oxidation in Diet-Induced Obesity». In: *Journal of Biological Chemistry* 293 (June 2018), pp. 9604–9613. ISSN: 00219258. DOI: 10.1074/jbc.RA118.002838.

[6] Honglei Wang and Wenhai Feng. «Current Status of Porcine Reproductive and Respiratory Syndrome Vaccines». In: *Vaccines* 12 (Dec. 10, 2024). ISSN: 2076-393X. DOI: 10.3390/vaccines12121387.

[7] Shih-Chia Tso et al. «Structure-Guided Development of Specific Pyruvate Dehydrogenase Kinase Inhibitors Targeting the ATP-binding Pocket». In: *Journal of Biological Chemistry* 289 (Feb. 2014), pp. 4432–4443. ISSN: 00219258. DOI: 10.1074/jbc.M113.533885.

[8] Shuo Zhang et al. «HSP90 Inhibitor 17-AAG Attenuates Nucleus Pulposus Inflammation and Catabolism Induced by M1-Polarized Macrophages». In: *Frontiers in Cell and Developmental Biology* 9 (Jan. 4, 2022). ISSN: 2296-634X. DOI: 10.3389/fcell.2021.796974.

[9] Shengming Ma et al. «PRRSV Subverts Host Programmed Cell Death Network for Immune Evasion». In: *Virulence* 17 (Dec. 31, 2026). ISSN: 2150-5594, 2150-5608. DOI: 10.1080/21505594.2026.2655108.

[10] Youle Zheng et al. «Inhibition of PRRSV Replication by Fangchinoline and Cepharanthine from Medicinal Herbs through Targeting of the CD163 Protein». In: *Veterinary Microbiology* 306 (July 2025). ISSN: 03781135. DOI: 10.1016/j.vetmic.2025.110536.

[11] Tongtong Wang et al. «Hyperoside Inhibits PRRSV Proliferation via the TLR4/NF- B and P62-Nrf2-Keap1 Signaling Pathways, Mediating Inflammation and Autophagy». In: *Microbiology Spectrum* 13 (Aug. 5, 2025), e03107–24. ISSN: 2165-0497. DOI: 10.1128/spectrum.03107-24.

[12] Zhilong Zhang et al. «The Effect of Matrine and Glycyrrhizic Acid on Porcine Reproductive and Respiratory Syndrome Virus in Vitro and in Vivo». In: *Virology Journal* 21 (July 4, 2024). ISSN: 1743-422X. DOI: 10.1186/s12985-024-02415-w.

AMERICAN SOCIETY FOR MICROBIOLOGY | Journal of Virology

| Veterinary Microbiology | Full-Length Text

Small-molecule PS10 inhibits PRRSV replication by targeting HSP90 and multiple viral non-structural proteins

Yongjie Chen,[1] Jingxing Wang,[1] Haotong Lu,[1] Zishen Chen,[1] Baoying Huang,[1] Chunhe Guo[1]

AUTHOR AFFILIATION See affiliation list on p. 20.

ABSTRACT Livestock production is vital to global food security but faces major threats from pathogens such as porcine reproductive and respiratory syndrome virus (PRRSV), which causes substantial economic losses. The genetic diversity of PRRSV and limited cross-protection among strains complicate vaccination strategies, highlighting the urgent need for effective antiviral treatments. In this study, we screened a compound library and identified 2-[(2,4-dihydroxyphenyl) sulfonyl] isoindoline-4,6-diol (designated PS10) as a potent inhibitor of PRRSV replication. PS10 exhibited dose-dependent antiviral effects in both Marc-145 cells and primary porcine alveolar macrophages, with efficacy independent of the viral strain. Further mechanistic studies revealed that PS10 acts specifically during the replication phase of the viral life cycle. Notably, PS10 significantly suppressed PRRSV infection-induced heat shock protein 90 (HSP90) expression, a critical host factor for viral replication. This suppression not only impaired viral propagation but also attenuated the production of pro-inflammatory cytokines. Furthermore, PS10 selectively reduced the abundance of multiple viral non-structural proteins (nsp2, nsp3, nsp10, and nsp11). The binding of PS10 to these proteins was confirmed by molecular docking and cellular thermal shift assays, which underlie the observed inhibition. This study not only expands our understanding of PS10's antiviral mechanisms but also provides new insights into host factor regulation of viral replication, offering potential avenues for developing broad-spectrum antiviral therapies.

IMPORTANCE Porcine reproductive and respiratory syndrome virus (PRRSV) causes substantial economic losses to the global swine industry. Current vaccines often lack cross-protection against heterologous strains, underscoring the need for broad-spectrum alternatives. We identified PS10 through compound screening as a potent inhibitor of PRRSV replication with low cytotoxicity. Mechanistically, PS10 significantly suppressed virus-induced expression of heat shock protein 90 (HSP90). This suppression not only inhibited viral propagation but also reduced pro-inflammatory cytokine production. Furthermore, PS10 reduced the levels of multiple viral non-structural proteins (nsp2, nsp3, nsp10, and nsp11). The binding of PS10 to these proteins was confirmed by molecular docking and cellular thermal shift assays. Taken together, our results suggest that PS10 is a promising candidate for controlling PRRSV infection and may provide a foundation for developing broad-spectrum antiviral agents.

KEYWORDS PRRSV, PS10, HSP90, viral non-structural proteins

As a primary source of meat in China, pork plays a vital role in the national diet and agricultural economy. However, the emergence and re-emergence of infectious diseases have posed serious challenges to the global swine industry. Viral diseases, in particular, threaten the sustainable development of pig farming and food security due to their high contagiousness and potential for widespread transmission (1, 2). Among these, porcine reproductive and respiratory syndrome (PRRS), caused by the PRRS virus (PRRSV),

Editor Rebecca Ellis Dutch, University of Kentucky College of Medicine, Lexington, Kentucky, USA

Address correspondence to Chunhe Guo, guochunh@mail.sysu.edu.cn.

Yongjie Chen, Jingxing Wang, and Haotong Lu contributed equally to this article. Author order was determined by increasing seniority.

The authors declare no conflict of interest.

Received 12 December 2025
Accepted 25 January 2026
Published 18 February 2026

Copyright © 2026 Chen et al. This is an open-access article distributed under the terms of the Creative Commons Attribution 4.0 International license.

Downloaded from https://journals.asm.org/journal/jvi on 25 February 2026 by 147.162.241.196.

is one of the most significant viral threats (3, 4). First identified in the United States in 1987, PRRS has spread worldwide, severely constraining pig production and causing substantial economic losses (5–7). PRRSV is an enveloped virus containing a single-stranded, positive-sense RNA genome approximately 15 kb in length. The genome comprises at least 11 open reading frames that encode 12 non-structural proteins (nsps) essential for viral replication, along with eight structural proteins required for virion assembly (8). Although pigs of all ages are susceptible to PRRSV infection, the most severe clinical outcomes are observed in pregnant sows and neonatal piglets (9). The virus exhibits specific tropism for macrophages, particularly porcine alveolar macrophages (PAMs), where it replicates before disseminating to lymphatic tissues and the lungs, thereby inducing respiratory symptoms. *In vitro*, it is capable of infecting the African green monkey kidney cell line (MA-104) and its derivative cell lines, such as Marc-145 (10).

PRRSV, as an RNA virus, exhibits characteristically high mutation rates due to the absence of proofreading mechanisms in its RNA-dependent RNA polymerase (11). This enables the virus to evolve rapidly, creating numerous genetic variants and resulting in extensive genetic and antigenic diversity among strains and leading to poor cross-protection between heterologous strains. Coupled with its immune evasion ability, current vaccines often fail to provide broad and lasting protection (12, 13). Given the limitations of these vaccines, small-molecule antiviral compounds are gaining attention as potential therapeutic alternatives for PRRSV control. These compounds can be specifically designed to target critical viral proteins or host factors. For example, small-molecule inhibitors can bind to the viral protease, blocking the processing of the viral polyprotein and inhibiting replication (14–16). Alternatively, other inhibitors may target essential host proteins involved in viral replication pathways (17, 18). Importantly, as long as target sites remain conserved across strains, these compounds can overcome viral variability. Therefore, screening for such compounds offers a promising strategy against PRRSV. Our experimental data demonstrate that the small-molecule 2-[(2,4-dihydroxyphenyl) sulfonyl] isoindoline-4,6-diol (PS10) significantly inhibits PRRSV replication, although its antiviral mechanism remains to be elucidated. Interestingly, PS10 has been previously identified as a novel ATP-competitive broad-spectrum pyruvate dehydrogenase kinase (PDK) inhibitor with demonstrated therapeutic potential for diabetic cardiomyopathy (19). Recent studies have also identified heat shock protein 90 (HSP90) as a binding target of PS10 (20). However, the function of PS10 in viral infection processes, particularly its antiviral mechanisms against PRRSV, remains unexplored. Further exploration of PS10's inhibitory effects on PRRSV replication may not only reveal novel antiviral mechanisms but also provide valuable insights for developing effective PRRSV control strategies.

In our research, through compound library screening, we identified PS10 as a potent inhibitor of PRRSV infection. Our mechanistic investigation revealed that PS10 inhibits PRRSV-induced HSP90 expression, which interferes with viral replication and reduces pro-inflammatory cytokine production. Additionally, PS10 was shown to selectively target and decrease the protein abundance of several viral nsps (nsp2, nsp3, nsp10, and nsp11). Furthermore, the interaction between PS10 and these nsps may contribute to their inhibition. These results highlight the potential of targeting both host HSP90 and viral nsps as a novel antiviral approach against PRRSV.

RESULTS

PS10 significantly inhibits PRRSV infection in Marc-145 cells

Small-molecule compound screening has been widely employed to identify inhibitors and therapeutic candidates for the prevention and treatment of diverse viral infections. To identify PRRSV inhibitors, Marc-145 cells were pretreated with compounds (10 µM) for 2 h before infection with luciferase-expressing PRRSV at a multiplicity of infection (MOI) of 0.5. Measurement of Gluc activity at 24 h post-infection (hpi) showed that PS10 significantly reduced Gluc expression, indicating strong anti-PRRSV activity (Fig. 1A). To

Downloaded from https://journals.asm.org/journal/jvi on 25 February 2026 by 147.162.241.196.

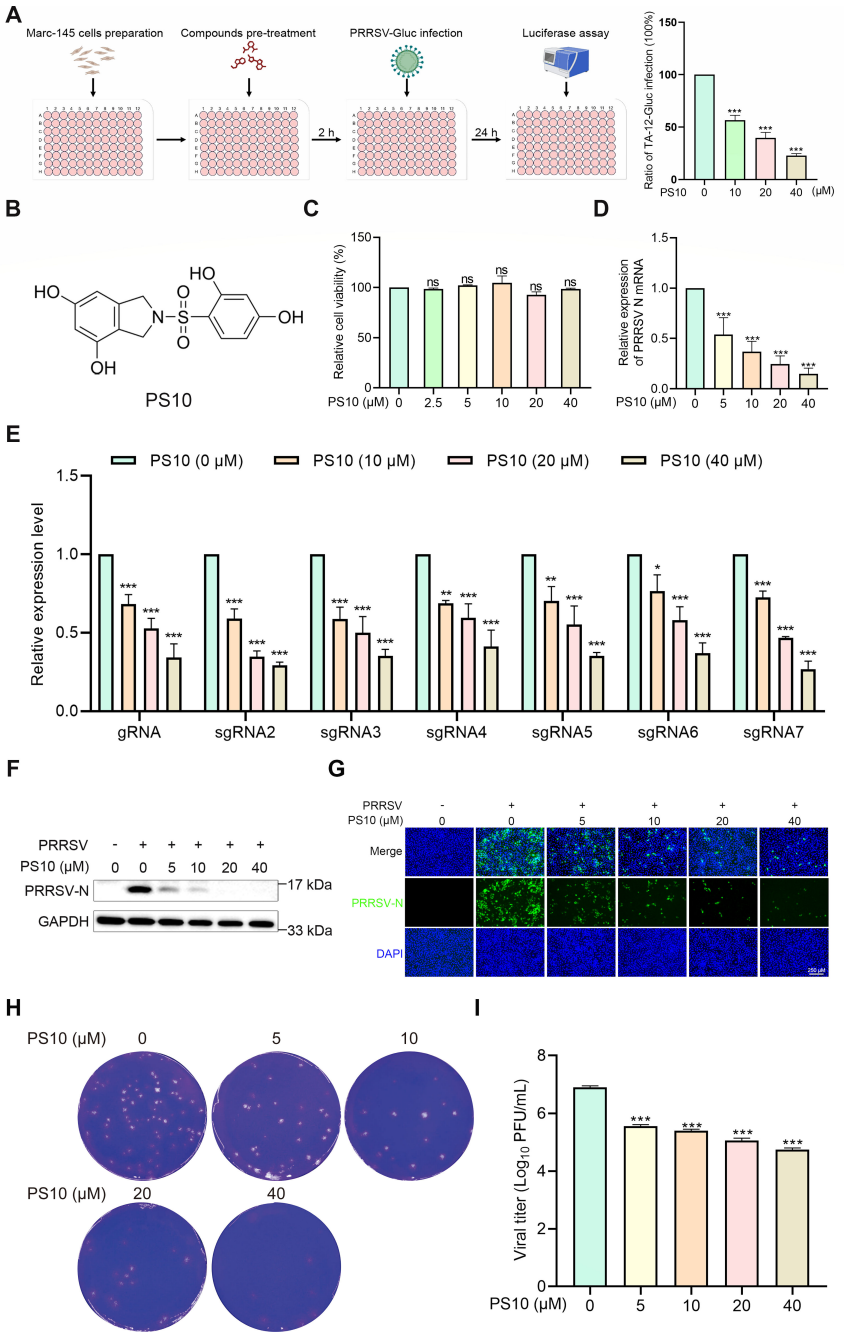


FIG 1 PS10 inhibits PRRSV infection in Marc-145 cells in a dose-dependent manner. (A) Design schematic of the compound screening experiment against PRRSV infection. Marc-145 cells were pre-incubated with the compound for 2 h and then infected with rTA-Gluc2 for 24 h. Culture supernatants were collected, and viral load was quantified using a microplate reader. (B) Chemical structure of PS10. (C) After 24 h of treatment with PS10 at the indicated concentrations, the cytotoxicity of PS10 on Marc-145 cells was assessed using a CCK-8 assay. (D-I) Marc-145 cells were treated with PS10 for 2 h and then infected with PRRSV CH-1a (MOI = 0.5). After 24 h, cells and supernatants were harvested. Viral RNA levels were measured by RT-qPCR (D and E). Viral N protein expression was analyzed by Western blotting (F) or immunofluorescence assay (IFA) (G). Virus titers in the supernatants were determined by plaque assay on Marc-145 cells (H and I). ***$P < 0.001$; **$P < 0.01$; *$P < 0.05$; ns: not significant.

exclude potential cytotoxic effects on viral infection, we first evaluated the impact of PS10 on Marc-145 cell viability using a CCK-8 assay (Fig. 1B). No significant cytotoxicity was observed at PS10 concentrations ≤ 40 μM (Fig. 1C). We next examined the antiviral

Downloaded from https://journals.asm.org/journal/jvi on 25 February 2026 by 147.162.241.196.

activity of PS10 against the PRRSV CH-1a strain. Although PS10 inhibited the mRNA levels of PRRSV N in a dose-dependent manner (Fig. 1D), the primers used targeted the N gene sequence and thus could not distinguish between genomic RNA (gRNA) and nested subgenomic mRNAs (sgmRNAs). To dissect its specific effect, we employed targeted assays for viral RNA synthesis and found that PS10 significantly suppressed the levels of both gRNA and sgmRNA (Fig. 1E). These results demonstrate that PS10 inhibits not only viral genomic replication but also subgenomic transcription. PS10 also reduced the level of the PRRSV N protein (Fig. 1F and G). Correspondingly, viral titers were significantly reduced in a dose-dependent manner compared to the control group (Fig. 1H and I). We further investigated the antiviral efficacy of PS10 at different time points during PRRSV infection. The results demonstrated that PS10 consistently suppressed both mRNA and protein levels of the PRRSV N across all tested time points (Fig. 2A through C). Furthermore, plaque assays confirmed that PS10 significantly reduced viral titers at each infection time point examined (Fig. 2D and E). Collectively, these data demonstrate that PS10 significantly inhibits PRRSV replication in Marc-145 cells.

PS10 suppresses PRRSV infection in PAMs

Since PAMs are the primary target cells for PRRSV infection, we investigated whether PS10 could also inhibit PRRSV replication in PAMs. Initial cytotoxicity assessment revealed no significant cytotoxic effects of PS10 on PAMs at concentrations ≤ 40 µM (Fig. 3A). Subsequently, we assessed the antiviral effect of PS10 against PRRSV JXA1 infection in PAMs. The results demonstrated that PS10 treatment significantly reduced the viral mRNA levels (Fig. 3B), N protein abundance (Fig. 3C), and progeny virus production (Fig. 3D and E) in a dose-dependent manner, indicating that PS10 can effectively inhibit PRRSV infection in PAMs as well.

Antiviral efficacy of PS10 against PRRSV infection under different treatment regimens

To evaluate the therapeutic potential of PS10 against PRRSV under different treatment modalities, we performed time-of-addition experiments by administering PS10 at three distinct stages: pre-treatment (2 h prior to viral infection), co-treatment (simultaneous with viral inoculation), and post-treatment (2 h after infection) (Fig. 4A). The results demonstrated that all three treatment modalities significantly suppressed both mRNA and protein expression levels of the PRRSV N (Fig. 4B and C), as well as a reduction in viral titers (Fig. 4D) and N protein fluorescence intensity (Fig. 4E). Notably, pre-treatment exhibited the strongest suppression of PRRSV, followed by co-treatment, with post-treatment showing the least effectiveness (Fig. 4B through E). These results demonstrate that PS10 achieves maximal antiviral activity when administered prior to viral infection.

PS10 does not directly interact with PRRSV virions

Some antiviral drugs inactivate viruses by disrupting virion integrity, thereby reducing the number of infectious particles and impairing viral entry (21). To investigate whether PS10 directly targets PRRSV particles, we incubated the virus with varying concentrations of PS10 in basal medium at 37°C for 2 h. After ultrafiltration to remove unbound PS10, the treated virions were resuspended in fresh medium and used to infect Marc-145 cells (Fig. 5A). Infection efficiency was quantified by measuring viral N protein expression and progeny virus production at 24 hpi. Notably, PRRSV pre-incubated with PS10 showed no significant reduction in infectivity compared to the control group (Fig. 5B through F), indicating that PS10 does not directly interact with or destabilize PRRSV virions. These results suggest that PS10's antiviral mechanism targets host or viral replication factors rather than structural components of the virus particle.

Downloaded from https://journals.asm.org/journal/jvi on 25 February 2026 by 147.162.241.196.

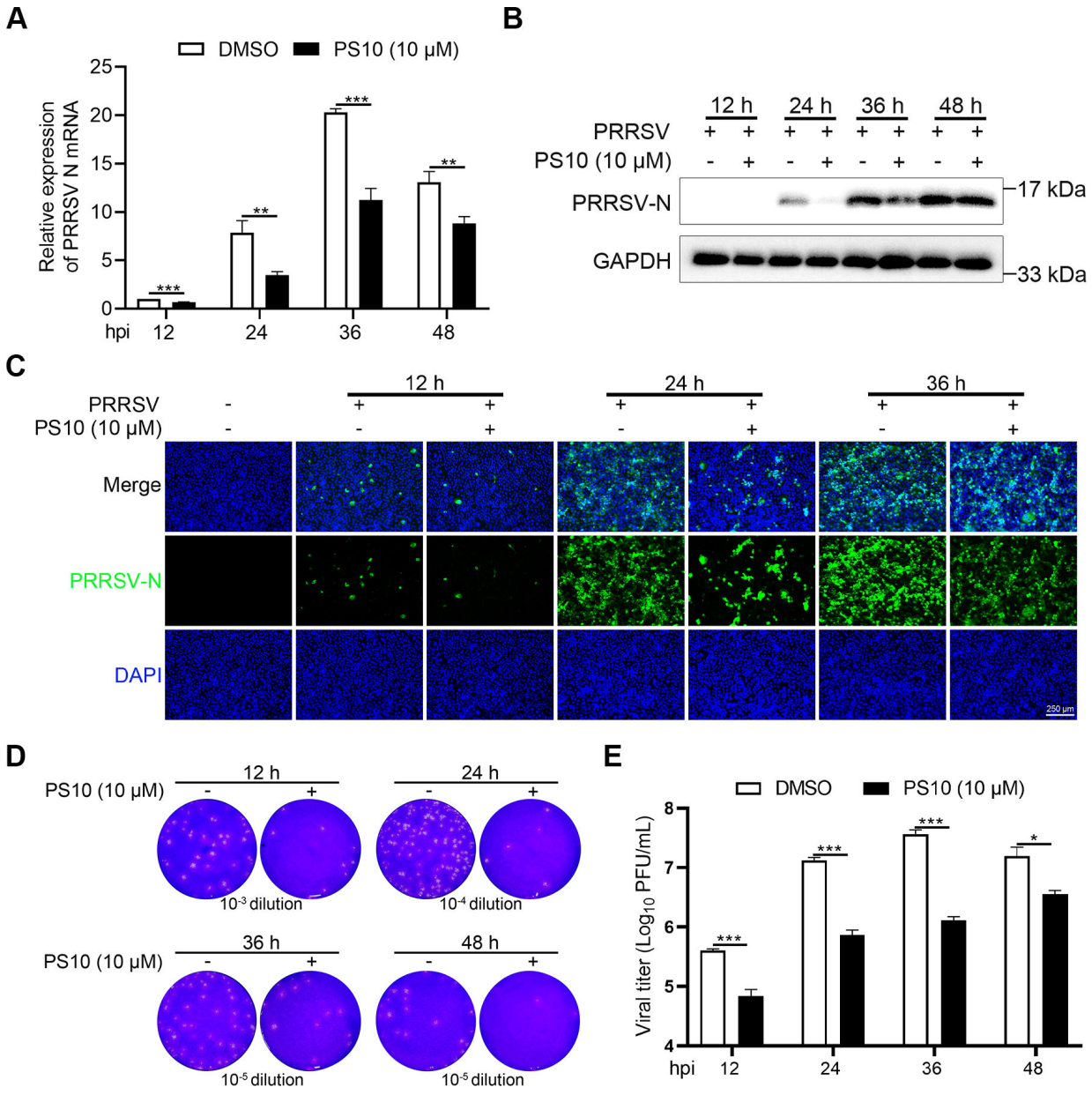


FIG 2 Time-dependent inhibition of PRRSV replication by PS10 in Marc-145 cells. (A–E) Marc-145 cells were treated with PS10 (10 μM) for 2 h and then infected with PRRSV CH-1a (MOI = 0.5) at the indicated time points, after which cells and supernatants were harvested for analysis. Viral RNA levels were measured by RT-qPCR (A). Viral N protein expression was analyzed by Western blotting (B) or IFA (C). Virus titers in the supernatants were determined by plaque assay on Marc-145 cells (D and E). ***$P < 0.001$; **$P < 0.01$; *$P < 0.05$; ns: not significant.

PS10 broadly suppresses the replication of diverse PRRSV strains

The substantial genetic diversity among PRRSV strains severely compromises the efficacy of current vaccines and poses significant challenges for disease control. To evaluate whether PS10 broadly inhibits the replication of diverse PRRSV strains, cells were treated with varying doses of PS10 followed by infection with multiple PRRSV-2 isolates (JXA1, SD16, TA-12, WUH3, and NADC30). The results demonstrated that PS10 treatment induced dose-dependent reductions in viral N protein levels across all strains tested (Fig. 6A through E). Consistent with these findings, quantitative fluorescence intensity analysis revealed significantly diminished PRRSV N protein signals (Fig. 6F through J). Furthermore, we evaluated PS10 against the PRRSV-1 strain BJEU06-1. Notably, PS10 also exhibited significant inhibitory activity, markedly reducing the N protein expression of

Downloaded from https://journals.asm.org/journal/jvi on 25 February 2026 by 147.162.241.196.

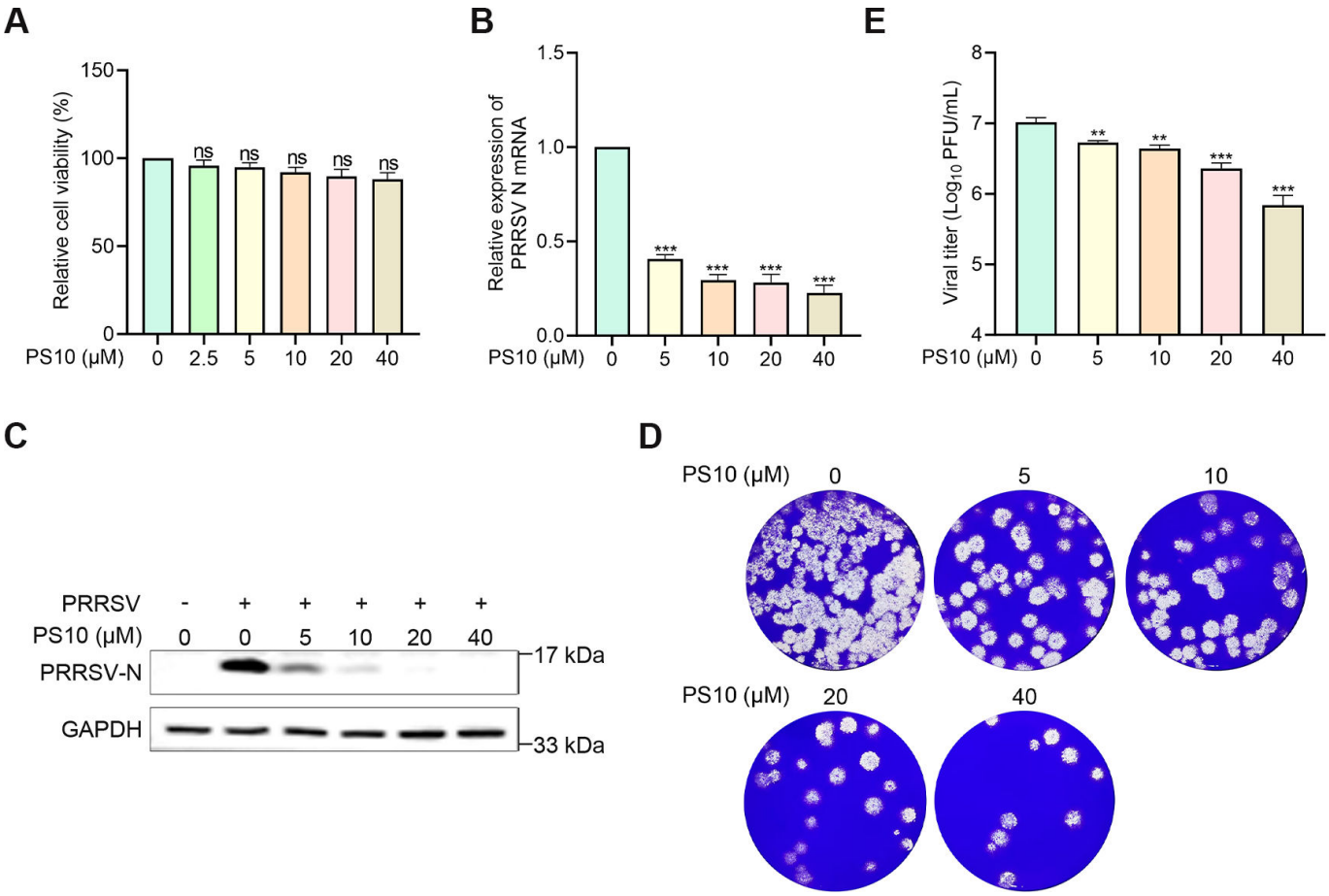


FIG 3 PS10 suppresses PRRSV infection in PAMs. (A) The viability of PAMs treated with the indicated concentrations of PS10 for 24 h was assessed using a CCK-8 assay. (B–E) PAMs were treated with PS10 for 2 h and then infected with PRRSV JXA1 (MOI = 0.5) for 24 h, after which cells and supernatants were harvested for analysis. Viral N mRNA and protein levels were quantified by RT-qPCR and Western blotting, respectively (B and C). Virus titers in the supernatants were determined by plaque assay on Marc-145 cells (D and E). ***$P < 0.001$; **$P < 0.01$; *$P < 0.05$; ns: not significant.

this strain (Fig. 6K and L). Collectively, these results indicate that PS10 exhibits broad-spectrum antiviral activity against diverse PRRSV strains.

PS10 specifically inhibits the replication stage of the PRRSV life cycle

The PRRSV life cycle primarily consists of four stages: adsorption, internalization, replication, and release. To investigate the mechanism of PS10 against PRRSV, we systematically examined its effects on each phase of the viral life cycle (Fig. 7A). Quantification of PRRSV N mRNA indicated that PS10 affected neither viral adsorption nor internalization (Fig. 7B and C). Plaque assays further confirmed that PS10 had no impact on the viral release process (Fig. 7E and F). In contrast, viral RNA quantification revealed that PS10 significantly inhibited the replication stage of PRRSV (Fig. 7D). These findings demonstrate that PS10 specifically inhibits the replication stage of PRRSV without affecting viral adsorption, internalization, or release.

PS10 suppresses PRRSV-induced HSP90 expression

Small-molecule compounds can modulate target protein expression through direct binding (17). Previous studies have indicated that PS10 binds to HSP90 (20). Given this binding relationship, it is crucial to explore whether there are other connections between PS10 and HSP90, as these potential connections might have implications for the biological processes involved. Additionally, previous studies have reported that

Downloaded from https://journals.asm.org/journal/jvi on 25 February 2026 by 147.162.241.196.

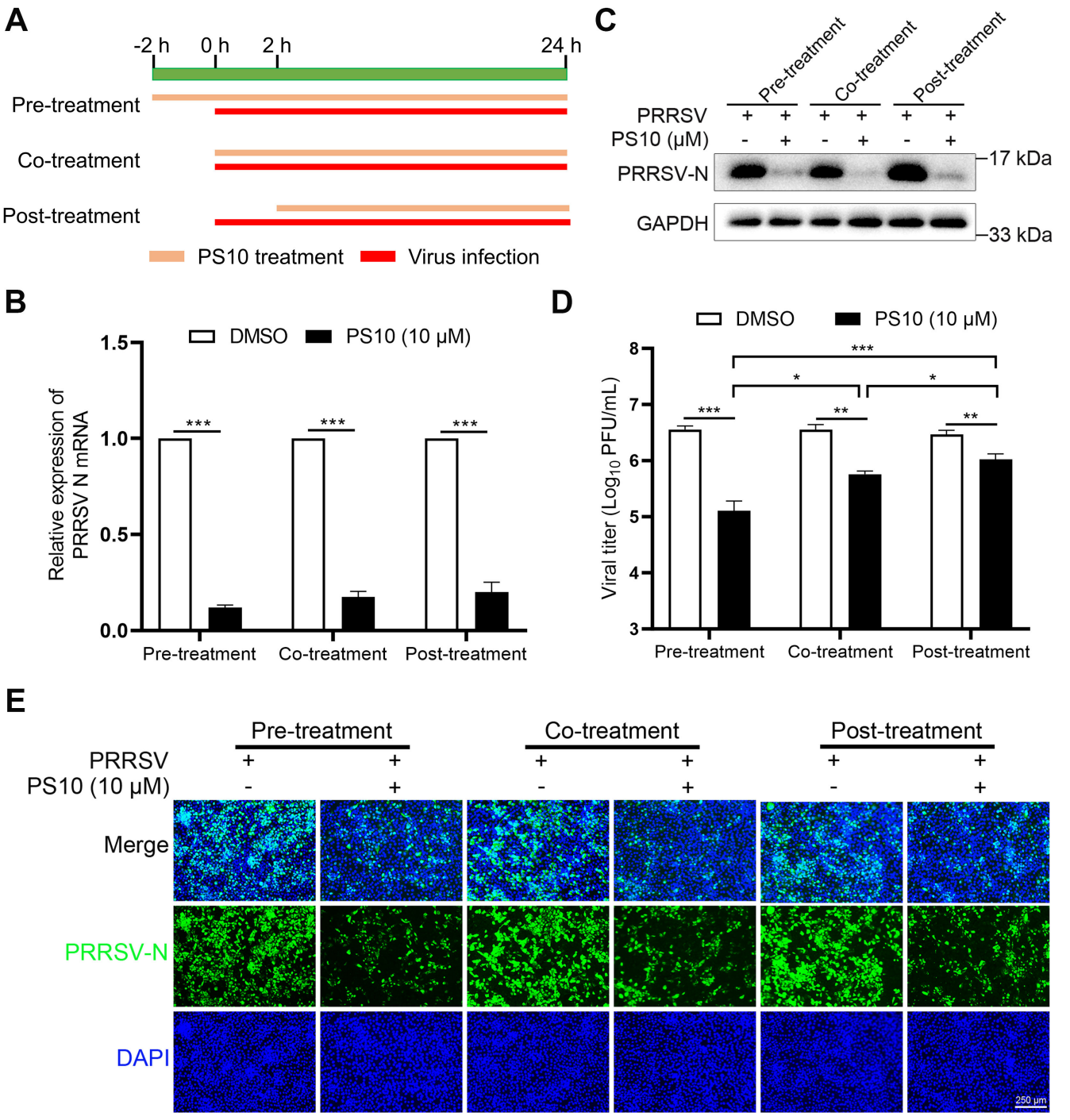


FIG 4 Antiviral efficacy of PS10 against PRRSV infection under different treatment regimens. (A) Schematic diagram of the three PS10 treatment protocols. (B–E) Marc - 145 cells were treated with PS10 (10 μM) before (pre - treatment), during (co - treatment), or after (post - treatment) infection with PRRSV CH - 1a (MOI = 0.5). Cells and supernatants were harvested 24 hpi for analysis. Viral RNA levels were quantified by RT-qPCR (B). Viral N protein expression was assessed by Western blotting (C). Virus titers in the supernatants were determined by plaque assay on Marc-145 cells (D). Viral N protein fluorescence intensity was analyzed by IFA (E). ***$P < 0.001$; **$P < 0.01$; *$P < 0.05$; ns: not significant.

HSP90 is essential for PRRSV replication (22). In light of this, we first examined the effect of PRRSV infection on HSP90 expression. The results demonstrated that PRRSV infection significantly enhanced the transcription of both HSP90AA1 and HSP90AB1 (Fig. 8A and B). Consistent with this, PRRSV infection also markedly upregulated the protein expression levels of total HSP90, HSP90AA1, and HSP90AB1 (Fig. 8C). We further assessed

Downloaded from https://journals.asm.org/journal/jvi on 25 February 2026 by 147.162.241.196.

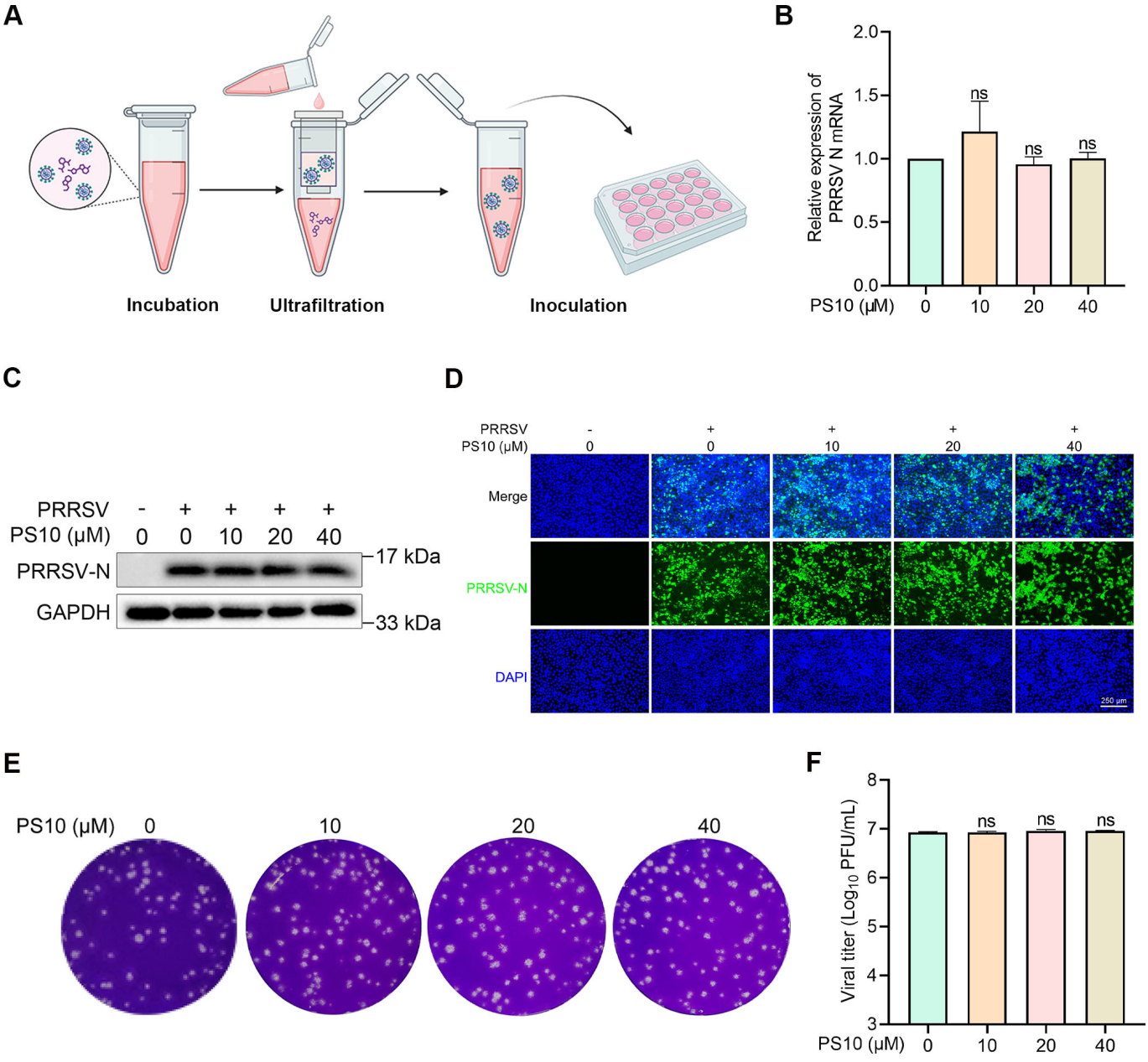


FIG 5 PS10 does not directly interact with PRRSV virions. (A) PRRSV CH - 1a virions were incubated with the indicated concentrations of PS10 in basal medium at 37°C for 2 h. The unbound compound was subsequently removed by ultrafiltration. (B–F) The recovered virions were resuspended and used to infect Marc - 145 cells. At 24 hpi, cells and supernatants were harvested. Viral N mRNA levels were quantified by RT-qPCR (B), and N protein expression was assessed by Western blotting (C) and IFA (D). Virus titers in the supernatants were determined by plaque assay on Marc-145 cells (E and F). ***$P < 0.001$; **$P < 0.01$; *$P < 0.05$; ns: not significant.

whether PS10 influences PRRSV-induced HSP90 expression. The results indicated that PS10 significantly suppressed the mRNA levels of HSP90AA1 and HSP90AB1 induced by PRRSV infection (Fig. 8D and E). Correspondingly, PS10 also markedly inhibited the PRRSV-induced protein expression of total HSP90, HSP90AA1, and HSP90AB1 (Fig. 8F). These results indicate that PS10 inhibits the up-regulation of HSP90 expression caused by PRRSV.

Downloaded from https://journals.asm.org/journal/jvi on 25 February 2026 by 147.162.241.196.

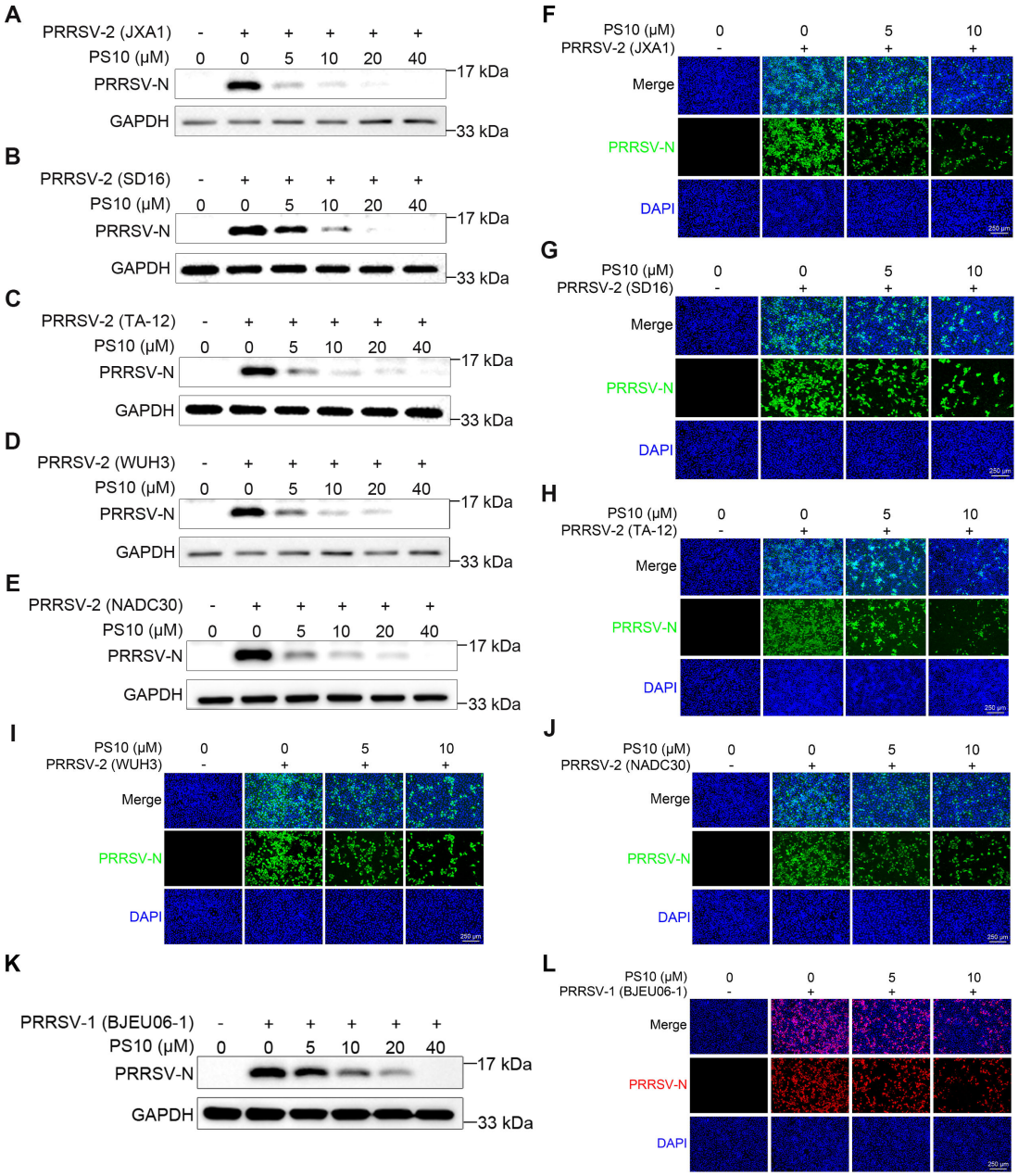


FIG 6 PS10 broadly suppresses the replication of diverse PRRSV strains. (A–J) Marc-145 cells were treated with PS10 for 2 h and then infected with PRRSV-2 strains (JXA1, SD16, TA-12, WUH3, and NADC30) at an MOI of 0.5 for 24 h. Samples were subsequently collected and analyzed by Western blotting (A–E) and IFA (F–J). (K and L) Marc-145 cells were treated with PS10 for 2 h and then infected with PRRSV-1 strain BJEU06-1 at an MOI of 0.5. After 24 h, samples were collected and analyzed by Western blotting (K) and IFA (L).

PS10 significantly restricts PRRSV proliferation by targeting and suppressing HSP90 function

Given the critical role of HSP90 in the life cycle of various viruses, we investigated whether PS10 affects viral replication by modulating HSP90 expression. We first assessed the impact of 17-AAG, a known HSP90 inhibitor, on the viability of Marc-145 cells. The results showed that 17-AAG concentrations below 10 μM had no significant effect on cell viability (Fig. 9A). We further evaluated the effect of 17-AAG on PRRSV replication. As the concentration of 17-AAG increased, both the PRRSV genomic copy number and the level of the viral N protein decreased in a dose-dependent manner (Fig. 9B through D). Concurrently, the protein levels of total HSP90, HSP90AA1, and HSP90AB1 were

Downloaded from https://journals.asm.org/journal/jvi on 25 February 2026 by 147.162.241.196.

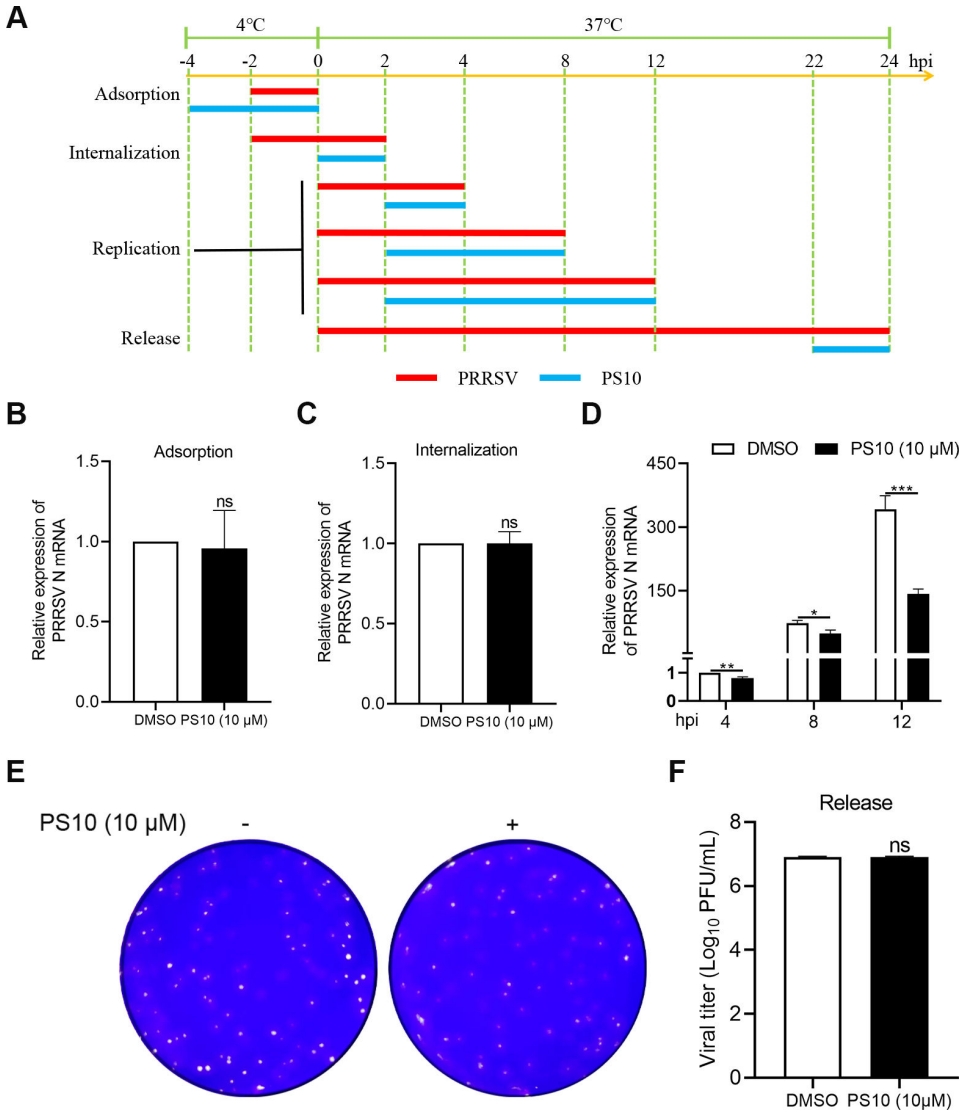


FIG 7 PS10 specifically inhibits the replication stage of the PRRSV life cycle. (A) Schematic of the viral binding, entry, replication, and release assays. (B) For the binding assay, Marc-145 cells were treated with PS10 (10 μM) at 4°C for 2 h and then infected with the PRRSV CH-1a (MOI = 10) at 4°C for 2 h. Viral N mRNA expression was quantified by RT-qPCR. (C) For the internalization assay, Marc-145 cells were infected with the PRRSV CH-1a (MOI = 10) at 4°C for 2 h and then treated with PS10 (10 μM) at 37°C for 2 h. Viral N mRNA expression was quantified by RT-qPCR. (D) For the replication assay, Marc-145 cells were infected with the PRRSV CH-1a (MOI = 0.5) at 37°C for 2 h and then treated with PS10 (10 μM) for the indicated durations. Viral N mRNA expression was quantified by RT-qPCR. (E and F) For the release assay, Marc-145 cells were infected with the PRRSV CH-1a (MOI = 0.5) at 37°C for 22 h and then treated with PS10 (10 μM) at 37°C for 2 h. Virus titers in the supernatants were determined by plaque assay on Marc-145 cells. ***$P < 0.001$; **$P < 0.01$; *$P < 0.05$; ns: not significant.

also reduced dose-dependently (Fig. 9C). To determine whether PS10 acts similarly, we compared its effects with 17-AAG, alone and in combination. Co-treatment did not affect cell viability (Fig. 9E). Notably, combined treatment with 17-AAG and PS10 led to the most substantial suppression of HSP90, HSP90AA1, and HSP90AB1 protein expression, and accordingly, the strongest inhibition of PRRSV replication (Fig. 9F through H). These results demonstrate that PS10 inhibits PRRSV replication by downregulating HSP90 expression.

Downloaded from https://journals.asm.org/journal/jvi on 25 February 2026 by 147.162.241.196.

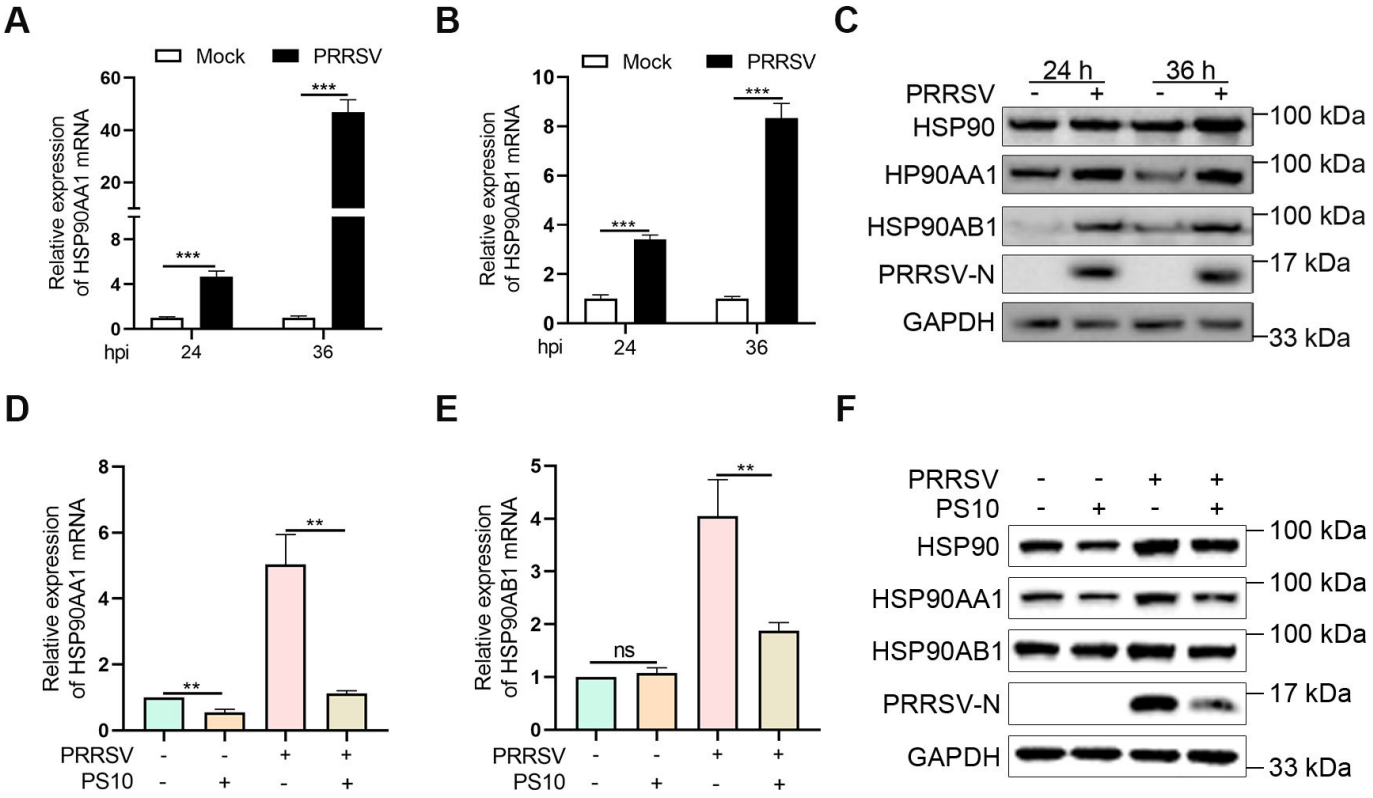


FIG 8 PS10 suppresses PRRSV-induced HSP90 expression. (A–C) Marc-145 cells were infected with PRRSV CH-1a (MOI = 0.5) for 24 h and 36 h. HSP90AA1 and HSP90AB1 mRNA levels were quantified by RT-qPCR (A and B), and HSP90, HSP90AA1, and HSP90AB1 protein levels were analyzed by Western blotting (C). (D–F) Marc-145 cells were pretreated with or without PS10 (10 μM) for 2 h and then infected with or without the PRRSV CH-1a (MOI = 0.5) for 24 h. HSP90AA1 and HSP90AB1 mRNA levels were measured by RT-qPCR (D and E), and HSP90, HSP90AA1, and HSP90AB1 protein levels were assessed by Western blotting (F). ***$P < 0.001$; **$P < 0.01$; *$P < 0.05$; ns: not significant.

PS10 suppresses the production of pro-inflammatory cytokines by downregulating HSP90 expression

HSP90 modulates inflammatory responses through multiple mechanisms (23). Given that PRRSV infection induces a storm of inflammatory cytokines in the lungs, contributing to respiratory symptoms, we investigated whether PS10 affects the production of inflammatory cytokines by regulating HSP90 expression. We first examined the effect of PS10 on PRRSV-induced expression of inflammatory factors. The results showed that PS10 significantly suppressed the mRNA expression of IL-6, IL-8, and TNF-α (Fig. 10A through C). Moreover, with increasing doses of PS10, the expression of IL-6, IL-8, and TNF-α mRNA also significantly decreased (Fig. 10D through F). Notably, the combined use of 17-AAG and PS10 inhibited the mRNA levels of IL-6, IL-8, and TNF-α more effectively than either compound alone (Fig. 10G through I). To rule out the possibility that the reduction in pro-inflammatory cytokines was secondary to decreased PRRSV infection, we tested PS10 and 17-AAG in uninfected HeLa cells stimulated with TNF-α. At a non-cytotoxic concentration, TNF-α induced cytokine production, which was significantly suppressed by both compounds (Fig. 10J through M). These results indicate that PS10 can inhibit inflammatory factors by suppressing HSP90 expression, rather than solely as a consequence of reduced PRRSV infection. We then asked whether suppressing inflammation itself affects PRRSV replication. Using the NF-κB inhibitor BAY 11-7082, we observed a dose-dependent reduction in PRRSV N-protein expression (Fig. 10N and O). Together, these findings demonstrate that PS10 inhibits the production of pro-inflammatory cytokines by downregulating HSP90 expression. This immunomodulatory action cooperates with direct antiviral mechanisms to suppress PRRSV infection.

Downloaded from https://journals.asm.org/journal/jvi on 25 February 2026 by 147.162.241.196.

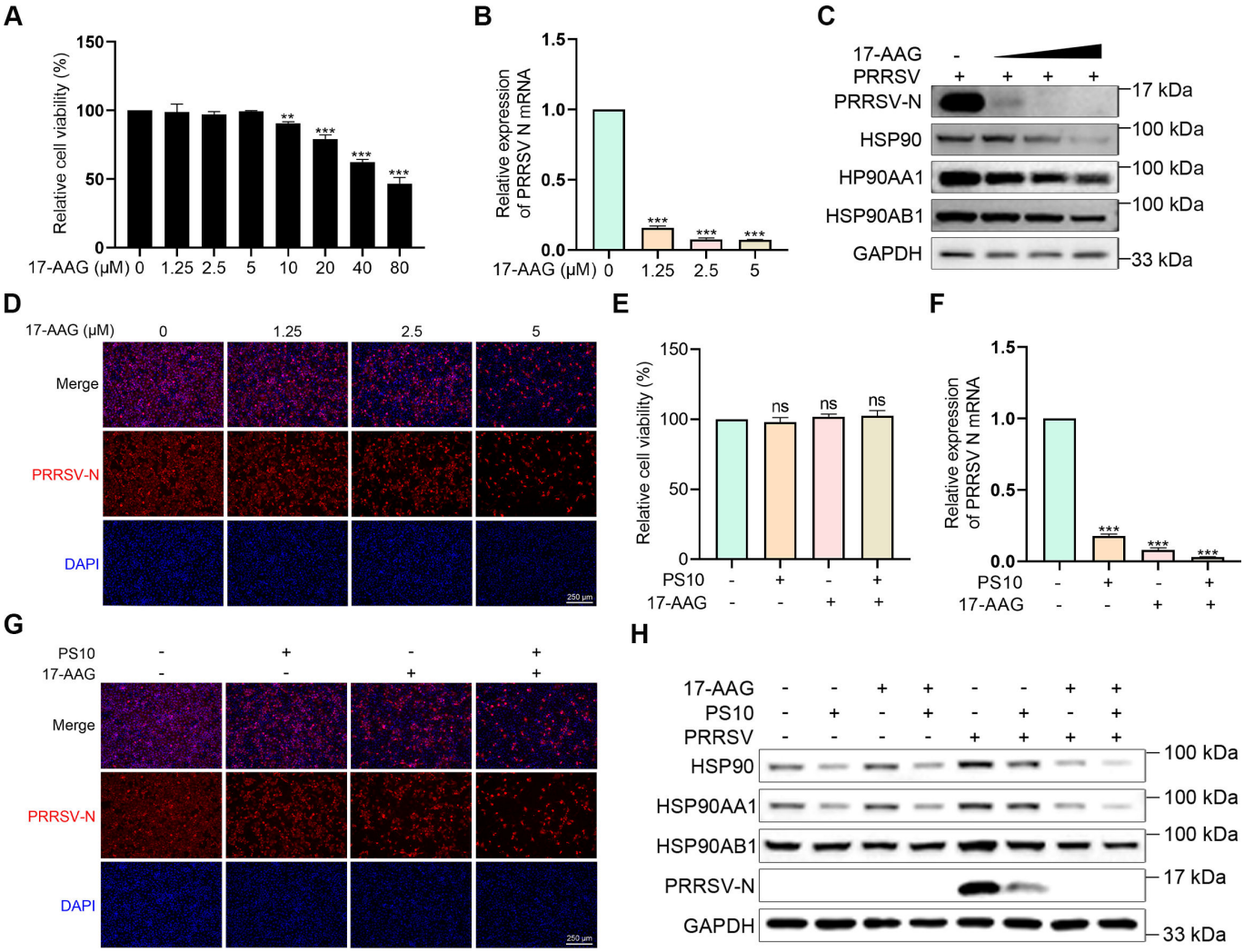


FIG 9 PS10 significantly restricts PRRSV proliferation by targeting and suppressing HSP90 function. (A) Viability of Marc-145 cells treated with the indicated concentrations of 17-AAG for 24 h was assessed using a CCK-8 assay. (B–D) Marc-145 cells were treated with 17-AAG for 2 h and then infected with PRRSV CH-1a (MOI = 0.5) for 24 h. Subsequently, samples were collected and analyzed by RT-qPCR (B), Western blotting (C), and IFA (D). (E) Viability of Marc-145 cells treated with PS10 (5 μM), 17-AAG (2.5 μM), or their combination for 24 h was assessed by CCK-8 assay. (F–H) Marc-145 cells were treated with PS10 (5 μM), 17-AAG (2.5 μM), or their combination for 2 h, and then infected with PRRSV CH-1a (MOI = 0.5) for 24 h. Mock-infected cells served as a control. Samples were collected and analyzed by RT-qPCR (F), IFA (G), and Western blotting (H). ***$P < 0.001$; **$P < 0.01$; *$P < 0.05$; ns: not significant.

PS10 specifically decreases the abundance of PRRSV nsp2, nsp3, nsp10, and nsp11

Our study demonstrates that PS10 inhibits the replication stage of the PRRSV life cycle. Given the crucial roles played by PRRSV nsps in viral replication, we investigated whether PS10 affects PRRSV replication by influencing the stability of these nsps. To rule out potential cytotoxic effects of PS10 on HEK293T cells, we first assessed its impact on cell viability. The results showed that PS10 at concentrations up to 40 μM did not affect HEK293T cell viability (Fig. 11A). Further investigation revealed that PS10 treatment specifically and significantly reduced the abundance of nsp2, nsp3, nsp10, and nsp11 proteins without affecting the expression of other nsps (Fig. 11B). Moreover, the inhibitory effect of PS10 on these proteins exhibited a clear dose-dependent manner, with higher concentrations leading to more pronounced suppression (Fig. 11C through F). In eukaryotic cells, protein degradation occurs primarily through three major pathways: the proteasome, autophagy, and apoptosis. To examine whether PS10-mediated reduction of nsps involves these mechanisms, we treated cells with specific

Downloaded from https://journals.asm.org/journal/jvi on 25 February 2026 by 147.162.241.196.

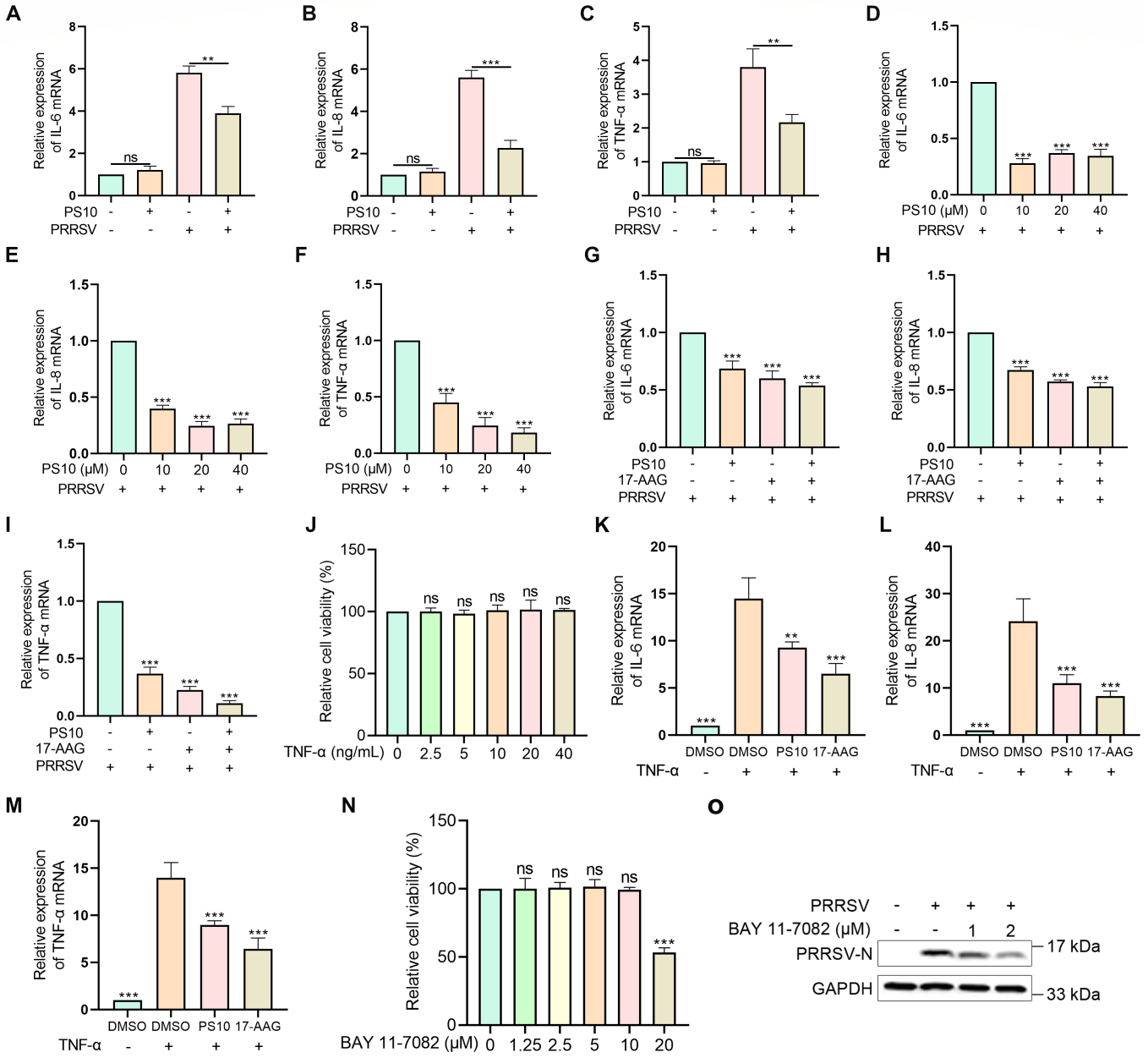


FIG 10 PS10 suppresses the production of pro-inflammatory cytokines by downregulating HSP90 expression. (A–C) Marc-145 cells were pretreated with or without PS10 (10 μM) for 2 h and then infected with or without the PRRSV CH-1a (MOI = 0.5) for 24 h. IL-6, IL-8, and TNF-α mRNA levels were measured by RT-qPCR. (D–F) Marc-145 cells were treated with different concentrations of PS10 for 2 h and then infected with the PRRSV CH-1a (MOI = 0.5) for 24 h. IL-6, IL-8, and TNF-α mRNA levels were measured by RT-qPCR. (G–I) Marc-145 cells were treated with PS10 (5 μM), 17-AAG (2.5 μM), or their combination for 2 h and then infected with PRRSV CH-1a (MOI = 0.5) for 24 h. IL-6, IL-8, and TNF-α mRNA levels were measured by RT-qPCR. (J) Viability of HeLa cells treated with indicated concentrations of TNF-α for 24 h was assessed by CCK-8 assay. (K–M) HeLa cells were treated with PS10 (40 μM) or 17-AAG (1 μM) for 12 h, followed by stimulation with TNF-α (10 ng/mL) for an additional 12 h. mRNA levels of IL-6, IL-8, and TNF-α were quantified by RT-qPCR. (N) Viability of Marc-145 cells treated with indicated concentrations of BAY 11-7082 for 24 h was assessed by CCK-8 assay. (O) Marc-145 cells were treated with different concentrations of BAY 11-7082 for 2 h and then infected with the PRRSV CH-1a (MOI = 0.5) for 24 h. N protein expression was analyzed by Western blotting. ***$P < 0.001$; **$P < 0.01$; *$P < 0.05$; ns: not significant.

inhibitors targeting the macroautophagy-lysosomal pathway (CQ), the ubiquitin-proteasome system (MG132), or caspase-mediated apoptotic (Z-VAD). We found that none of the inhibitors prevented PS10-induced reduction of nsp2 (Fig. 11G). In contrast, the reduced abundance of nsp3, nsp10, and nsp11 was partially rescued by these inhibitors (Fig. 11H through J). PS10 also reduced nsp2 and nsp10 levels during PRRSV infection

Downloaded from https://journals.asm.org/journal/jvi on 25 February 2026 by 147.162.241.196.

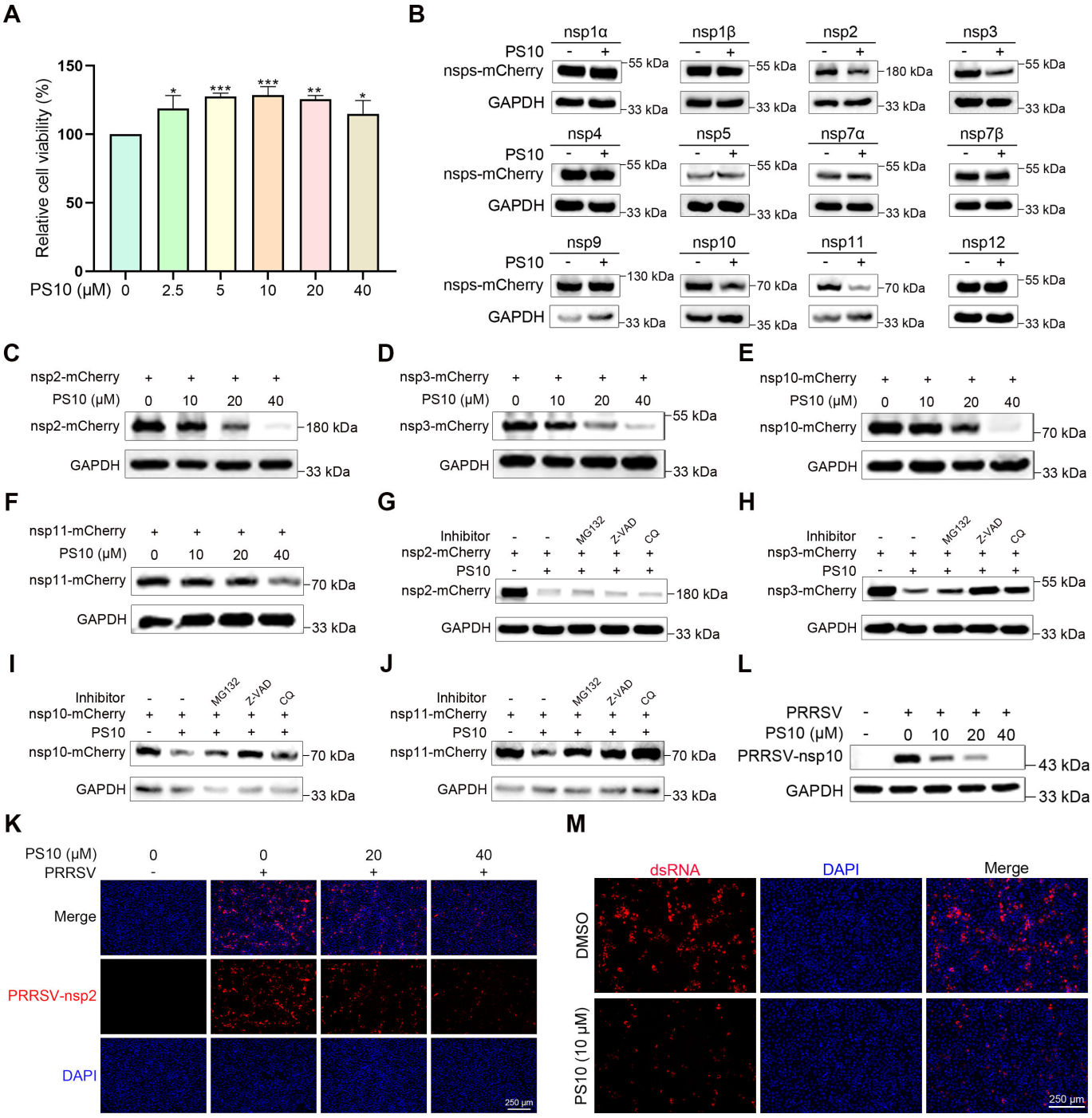


FIG 11 PS10 specifically reduces the abundance of PRRSV nsp2, nsp3, nsp10, and nsp11. (A) Viability of HEK-293T cells treated with the indicated concentrations of PS10 for 24 h was assessed using a CCK-8 assay. (B) HEK293T cells were transfected with plasmids encoding PRRSV nsps-mCherry. At 6 h post-transfection, cells were treated with PS10 (40 μM) or DMSO and harvested at 24 h for Western blot analysis of nsp protein levels. (C–F) HEK293T cells transfected with plasmids encoding individual nsp2, nsp3, nsp10, or nsp11 were treated with the indicated concentrations of PS10 at 6 h post-transfection. Cells were harvested at 24 h for Western blot analysis. (G–J) HEK293T cells were transfected with plasmids encoding individual nsp2, nsp3, nsp10, or nsp11. Cells were treated with PS10 (40 μM) or DMSO at 6 h and with corresponding inhibitors at 12 h post-transfection. All cells were harvested at 24 h for Western blot analysis. (K and L) Marc-145 cells were treated with PS10 for 2 h and then infected with PRRSV CH-1a (MOI = 0.5). After 24 h, samples were collected and analyzed by Western blotting (K) and IFA (L). (M) Marc-145 cells were pretreated with PS10 (10 μM) for 2 h and then infected with the PRRSV CH-1a (MOI = 0.5) for 12 h. Viral dsRNA was detected by IFA. ***$P < 0.001$; **$P < 0.01$; *$P < 0.05$; ns: not significant.

Downloaded from https://journals.asm.org/journal/jvi on 25 February 2026 by 147.162.241.196.

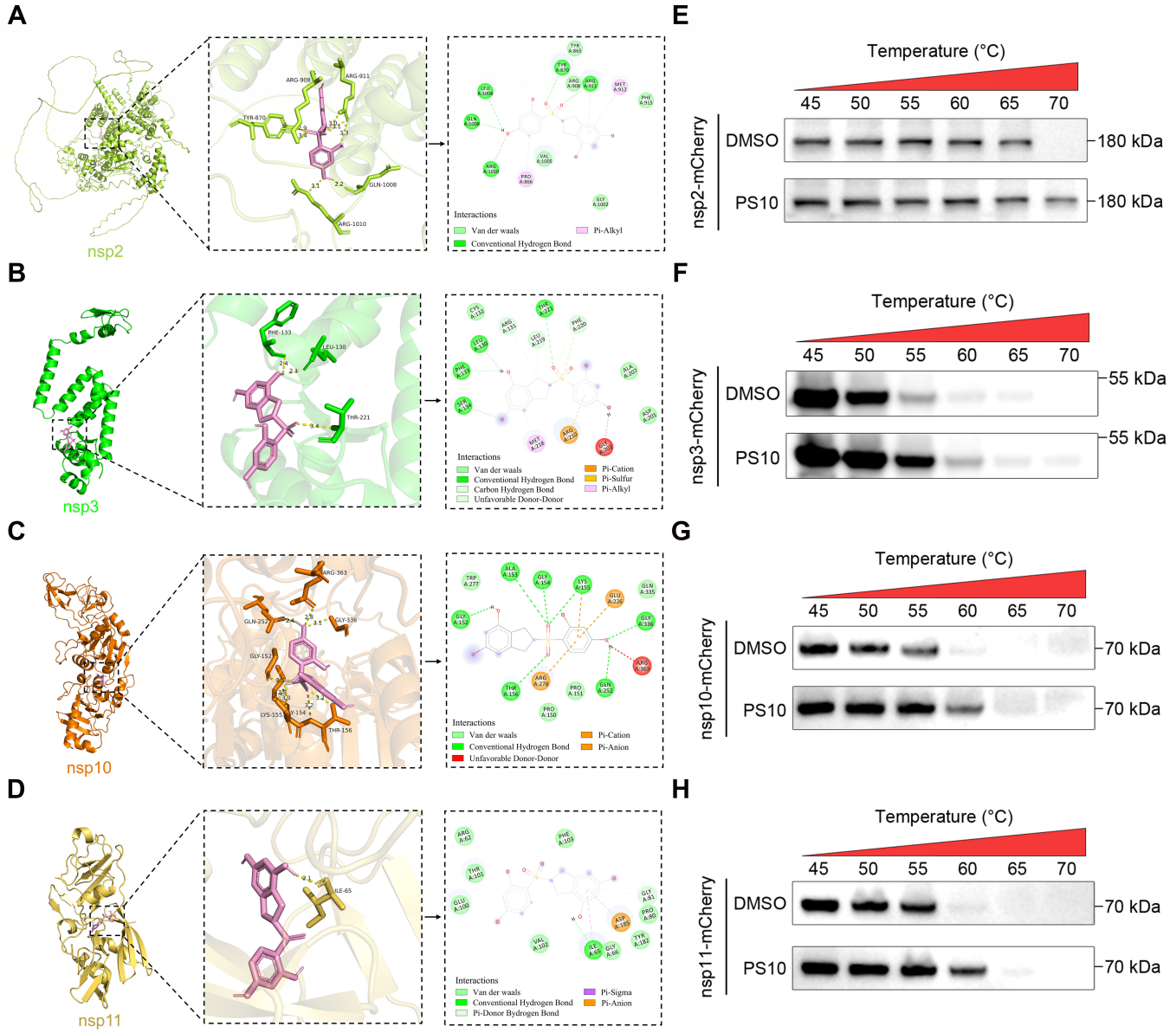


FIG 12 PS10 binds to PRRSV nsp2, nsp3, nsp10, and nsp11. (A–D) Ligand structures and protein structures were obtained from PubChem and AlphaFold3, respectively. Molecular docking was performed using CB-Dock2, and the results were visualized with Discovery Studio and PyMOL. (E–H) The cells were transfected with plasmids encoding viral proteins for 24 h, followed by lysis. Subsequently, the lysate was incubated with PS10 (40 µM) at 37°C for 30 min. The mixture was then transferred to a PCR machine and heated at different temperature gradients for 3 min, followed by three cycles of freeze-thawing in liquid nitrogen. After centrifugation, the supernatant was collected for SDS-PAGE analysis.

(Fig. 11K and L). Given that PS10 compromises the stability of key replicase subunits, including the essential replication-transcription complex (RTC) components nsp2 and nsp3, we hypothesized that it would interfere with the replication phase of the PRRSV life cycle. As double-stranded RNA (dsRNA) serves as a replication intermediate and is indicative of active viral replication, we investigated the impact of PS10 on dsRNA synthesis. Our results showed that treatment with PS10 significantly suppressed the formation of PRRSV dsRNA (Fig. 11M). Taken together, these results indicate that PS10 inhibits PRRSV replication by reducing the abundance of key nsps (nsp2, nsp3, nsp10, and nsp11).

Downloaded from https://journals.asm.org/journal/jvi on 25 February 2026 by 147.162.241.196.

PS10 binds to PRRSV nsp2, nsp3, nsp10, and nsp11

Given that PS10 affects the stability of nsp2, nsp3, nsp10, and nsp11, we hypothesized that PS10 might interact with these nsps. To evaluate this possibility, we first performed computational molecular docking to analyze potential interactions between PS10 and each target protein. The docking results indicated favorable binding interactions between PS10 and nsp2, nsp3, nsp10, and nsp11 (Fig. 12A through D). We further validated these interactions using cellular thermal shift assay (CETSA). Protein extracts from HEK293T cells expressing individual nsps were treated with PS10 (40 µM) or DMSO and subjected to a heat pulse. The results demonstrated that PS10 significantly enhanced the thermal stability of exogenously expressed nsp2, nsp3, nsp10, and nsp11 and delayed their heat-induced degradation (Fig. 12E through H). Collectively, these findings provide direct evidence that PS10 can physically bind to nsp2, nsp3, nsp10, and nsp11.

DISCUSSION

The increasing threat of emerging and re-emerging animal infectious diseases jeopardizes global livestock production, food security, and the sustainability of animal-sourced food systems (24). In China, pork plays a vital role in national food security (25). Porcine viral diseases persistently challenge swine industry development, and among these, PRRSV has become particularly detrimental due to its high genetic diversity, frequent mutations, and recombination events, which undermine current vaccine efficacy (26). Thus, effective therapeutic interventions against PRRSV infection are urgently needed. While vaccination remains a primary strategy, its limitations highlight the critical need for drug therapy (27, 28). Previous studies have identified several compounds with anti-PRRSV activity *in vitro* and *in vivo* (29–31). To expand the antiviral candidate pool, we performed systematic screening and identified PS10 as a novel inhibitor. PS10 showed low cytotoxicity in Marc-145 cells and PAMs and displayed potent anti-PRRSV activity *in vitro*. Given its low-cost profile and potent efficacy at low doses, PS10 is a promising candidate for targeted anti-PRRSV therapy. We observed that its inhibitory efficacy was somewhat lower in PAMs than in Marc-145 cells, likely due to inherent biological differences between cell types and the use of distinct PRRSV strains. Following PS10 treatment, we noted heterogeneous plaque sizes. High-throughput sequencing revealed a PS10-induced mutation in the PRRSV genome, which may attenuate viral replication or represent an adaptive, resistance-conferring change (data not shown). Certain antiviral agents can suppress replication by increasing viral mutagenesis (32).

Treatment regimen studies indicated that pre-treatment with PS10 had the strongest antiviral effect, while post-treatment was least effective. Time-course experiments further showed that PS10's inhibitory capacity diminished during later infection stages, suggesting prophylactic administration may be the optimal strategy for PRRSV control. Although some antiviral compounds act by directly inactivating viral particles (33), we found that PS10 does not directly interact with the virion. Given PRRSV's genetic diversity, we evaluated PS10 against multiple strains and observed broad-spectrum inhibitory activity. As an enveloped virus, PRRSV progresses through attachment, internalization, replication, and release (34, 35). Our mechanistic studies revealed that PS10 specifically disrupts the replication stage, likely by modulating host factors required for viral replication. Previous studies indicate HSP90 is a binding target of PS10 (20). HSP90 is a key molecular chaperone that supports the folding, stabilization, and nuclear transport of multiple viral proteins (36). It has been demonstrated that Carrimycin interacts with transmembrane protein B (TMEM41B) and induces its degradation via the proteasomal pathway (17). Based on this precedent, we investigated whether PS10 similarly modulates HSP90 expression. Our results showed that PS10 suppressed the PRRSV-induced expression of HSP90 and thereby inhibited viral replication. This aligns with the established role of HSP90 in the replication of diverse viruses, including PRRSV (22), African swine fever virus (ASFV) (37), herpes simplex virus type I (HSV-1) (38), and bluetongue virus (BTV) (39).

Downloaded from https://journals.asm.org/journal/jvi on 25 February 2026 by 147.162.241.196.

During PRRSV infection, the virus activates NF-κB to upregulate pro-inflammatory cytokines, contributing to the systemic hyperinflammatory response characteristic of PRRSV pathogenesis (40). Notably, HSP90 stabilizes IKK-β to sustain NF-κB signaling (41) and facilitates NLRP3 inflammasome activation (42). Consistent with this, the HSP90 inhibitor 17-AAG suppresses inflammatory cytokine production (43). We therefore hypothesized that PS10 might attenuate PRRSV-induced inflammation by suppressing HSP90 expression. Indeed, PS10 significantly inhibits pro-inflammatory cytokine production during PRRSV infection. In uninfected cells stimulated with TNF-α, both PS10 and 17-AAG reduced cytokine expression, confirming that the anti-inflammatory effect of PS10 is mediated, at least in part, through HSP90 downregulation and is not merely due to reduced viral infection. These results suggest that PS10 may also exert antiviral activity against other viruses by downregulating HSP90 expression.

Previous studies have established that multiple antiviral compounds inhibit viral replication by directly targeting viral proteins (44–46). In PRRSV, nsps play critical roles in viral replication and pathogenesis (47, 48). Since PS10 was found to specifically block the replication stage of PRRSV, we investigated its effects on nsps expression. PS10 significantly reduced levels of nsp2, nsp3, nsp10, and nsp11. Notably, the decrease in nsp3, nsp10, and nsp11 could be rescued by CQ, MG132, or Z-VAD, whereas nsp2 degradation was not reversed by any of these treatments, suggesting a distinct degradation mechanism. PS10 also suppressed nsp2 and nsp10 protein expression

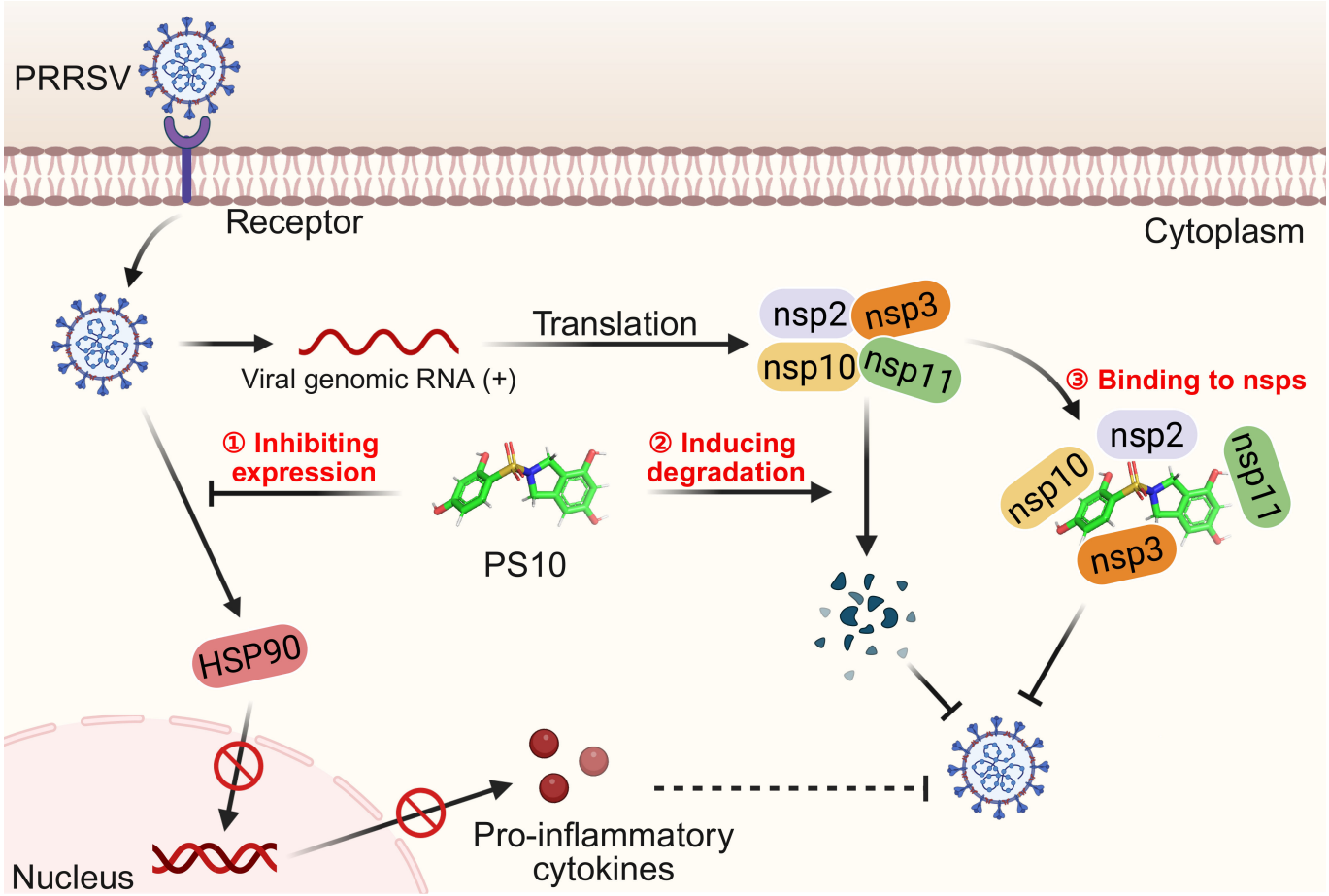


FIG 13 Schematic model illustrating the mechanism of PS10-mediated inhibition of PRRSV replication. Following receptor binding and entry into the host cell, PS10 inhibits the replication phase of the PRRSV life cycle. Specifically, (i) PS10 significantly suppresses PRRSV infection-induced expression of HSP90, thereby impairing viral propagation and attenuating pro-inflammatory cytokine production. (ii) PS10 can also selectively target and degrade multiple viral nsps, including nsp2, nsp3, nsp10, and nsp11. This targeted degradation constitutes the key mechanism underlying its antiviral activity. (iii) Furthermore, PS10 binds to these viral proteins, which may contribute to its inhibition of PRRSV replication.

Downloaded from https://journals.asm.org/journal/jvi on 25 February 2026 by 147.162.241.196.

during infection. These nsps perform key functions: nsp2 possesses PLP2 protease activity (49), nsp3 is a transmembrane protein essential for the replication-transcription complex (50), nsp10 functions as a helicase (11), and nsp11 exhibits endoribonuclease activity (14). Furthermore, CETSA confirmed interactions between PS10 and these nsps, a finding that was corroborated by molecular docking analysis. This binding may explain PS10's ability to suppress the expression of these proteins. These findings align with prior reports demonstrating that small molecules can exert antiviral effects through interactions with viral proteins (51–53). Interestingly, we also observed that PS10 treatment enhanced the viability of HEK-293T cells without affecting Marc-145 cells or PAMs. This cell type-specific pro-survival effect may be related to differences in basal metabolic or stress states and warrants further investigation.

In conclusion, our study demonstrates for the first time that PS10 functions as a critical antiviral agent, specifically against PRRSV. Its mechanism involves suppressing viral proliferation and mitigating inflammatory responses by downregulating HSP90 expression. Furthermore, PS10 interacts with PRRSV nsp2, nsp3, nsp10, and nsp11, which may contribute to its specific inhibition of these proteins (Fig. 13). These findings highlight PS10 as a promising lead compound for anti-PRRSV therapy. Moreover, its dual targeting of host and viral factors suggests potential broad-spectrum antiviral applications.

MATERIALS AND METHODS

Cells and viruses

HEK293T cells, Marc-145 cells, and HeLa cells were maintained in Dulbecco's modified Eagle's medium (DMEM; Bio-Channel, BC20250708) supplemented with 10% fetal bovine serum (FBS; ExCell Bio, FSP500). Primary porcine alveolar macrophages, the natural target cells for PRRSV infection, were isolated from 4-week-old PRRSV-negative piglets using established protocols and cultured in RPMI 1640 medium (Gibco) containing 10% FBS. The PRRSV-2 strains JXA1 (FJ548855.1), SD16 (JX087437.1), TA-12 (HQ416720.1), WUH3 (HM853673.2), NADC30 (MH500776), and CH-1a (AY032626.1), and the PRRSV-1 strain BJEU06-1 (GU047344.1) were used in this study. All viral stocks were propagated and titrated in Marc-145 cells.

Reagents and antibodies

The small-molecule PS10 (HY-121744), MG132 (HY-13259), chloroquine (CQ; HY-17589A), Z-VAD (HY-164388), and the NF-κB inhibitor BAY 11-7082 (HY-13453) were purchased from MedChemExpress. Tanespimycin (17-AAG; A220462) was obtained from AmBeed. Recombinant human TNF-α (300-01A) was purchased from Thermo Fisher Scientific. 4′,6-diamidino-2-phenylindole, dihydrochloride (DAPI; C0065, 1:1,000) was acquired from Solarbio, and polyethylenimine (PEI; G1802) was purchased from Servicebio. Anti-PRRSV N monoclonal antibody (JN0401, 1:3,000) was sourced from MEDIAN Diagnostics (Korea). Anti-GAPDH (60004-1-Ig, 1:5,000), Anti-mCherry-tag (26765-1-AP, 1:2,000), HRP-conjugated anti-mouse (SA00001-1, 1:10,000), and anti-rabbit (SA00001-2, 1:10,000) antibodies were acquired from Proteintech Group. Alexa Fluor 488-conjugated goat anti-mouse (4408, 1:1,000) antibodies, as well as Alexa Fluor 555-conjugated goat anti-mouse (4409, 1:1,000) antibodies, were purchased from Cell Signaling Technology. Furthermore, anti-HSP90 (F0283, 1:1,000), anti-HSP90AA1 (F0889, 1:1,000), and anti-HSP90AB1 (F1132, 1:1,000) were sourced from Selleck Chemicals.

Cytotoxicity assay

Cell viability was determined using the CCK-8 assay (GlpBio, GK10001). Marc-145 cells or PAMs were seeded in 96-well plates and treated with specified compounds for 24 h.

Downloaded from https://journals.asm.org/journal/jvi on 25 February 2026 by 147.162.241.196.

After treatment, 10 µL of CCK-8 reagent was added per well, followed by 1-h incubation. Absorbance was measured at 450 nm using a microplate reader.

RNA extraction and quantitative real-time PCR

Total RNA was extracted from Marc-145 cells or PAMs using TRIeasy Reagent (YEASEN, 10,606ES60) and reverse transcribed into cDNA with ABScript Neo RT Master Mix for qPCR with gDNA Remover (ABclonal, RK20433). Quantitative real-time PCR was conducted using BrightCycle Blue Universal SYBR Green qPCR Mix with UDG (ABclonal, RK21220) on the QuantStudio 3 Real-Time PCR system (Thermo Fisher Scientific). Relative gene expression was normalized to GAPDH (for Marc-145 or HeLa cells) or HPRT1 (for PAMs) and calculated using the $2^{-\Delta\Delta CT}$ method. All primer sequences are listed in Table S1.

Western blotting

Cells were lysed in RIPA buffer (Beyotime, P0013B) containing 1 mM PMSF (Solarbio, P0100) on ice for 30 min. Lysates were separated by SDS-PAGE and transferred to PVDF membranes (Merck Millipore, ISEQ00010). After blocking with 5% skim milk (Beyotime, P0216) for 2 h at room temperature, membranes were incubated with primary antibodies overnight at 4°C. Following three washes, membranes were probed with HRP-conjugated secondary antibodies for 1 h at room temperature. Protein signals were detected using an ECL kit (MeilunBio, MA0186-3).

Indirect IFA

Cells were fixed with 4% paraformaldehyde (Beyotime, P0099) for 15 min at room temperature, followed by permeabilization with 0.5% Triton X-100 (Beyotime, P0096) for 5 min. After three PBS washes, non-specific binding was blocked with 1% BSA (Beyotime, ST2249) for 1 h at room temperature. Primary antibody incubation was performed overnight at 4°C, followed by three PBS washes and 1-h incubation with fluorescent secondary antibodies at room temperature. Nuclei were counterstained with DAPI for 5 min before imaging with an inverted fluorescence microscope (Nikon ECLIPSE Ti2).

Viral titration by plaque assay

Marc-145 cells in six-well plates were infected with 10-fold serially diluted PRRSV for 1 h (with gentle agitation every 15 min). After removing the inoculum and washing with PBS, cells were overlaid with DMEM containing 1% low-melting agarose and 2% FBS. Following solidification, plates were incubated at 37°C with 5% CO_2 for 72 h. Plaques were visualized by crystal violet staining after agarose removal.

Direct PRRSV-PS10 interaction

PRRSV was incubated with increasing concentrations of PS10 for 2 h at 37°C to evaluate direct virion interaction. Virus-compound complexes were isolated by centrifugal filter devices (Pall, OD100C33). After three washes with basal medium to remove unbound PS10, purified virions were resuspended and inoculated onto Marc-145 cells for 24-h infectivity analysis.

Plasmid transfection and treatment

The plasmids expressing the nsps of PRRSV were stored in our laboratory. HEK-293T cells were seeded into 12-well plates. When the cell density reached approximately 80%, these plasmids were transfected into the cells using PEI. Six hours post-transfection, the cells were treated with or without PS10. Samples were collected at 24 h post-transfection for western blotting analysis.

Downloaded from https://journals.asm.org/journal/jvi on 25 February 2026 by 147.162.241.196.

Cellular thermal shift assay

HEK293 cells transfected with the corresponding plasmids for 24 h were lysed in NP-40 Lysis Buffer (Beyotime, P0013F). Aliquots (50 µL) of lysate were incubated with or without PS10 (40 µM) at 37°C for 30 min. Samples were then divided and heated at 45°C, 50°C, 55°C, 60°C, 65°C, and 70°C for 3 min, followed by three cycles of freezing in liquid nitrogen and thawing at 25°C. After being centrifuged at 12,000 × *g* for 20 min at 4°C, supernatants were carefully transferred to new tubes, mixed with loading buffer, boiled at 100°C for 10 min, and finally analyzed by western blotting.

Molecular docking

To investigate protein-small molecule interactions, molecular docking was performed. Ligand structures were acquired from PubChem (https://pubchem.ncbi.nlm.nih.gov), and protein structures were predicted using AlphaFold 3 (https://alphafoldserver.com/). Docking simulations were conducted with CB-Dock2 (https://cadd.labshare.cn/cb-dock2/), and resulting complexes were visualized using Discovery Studio and PyMOL.

Statistical analysis

Data were analyzed using GraphPad Prism 8. Pairwise comparisons were conducted using Student's t-test, while multi-group comparisons employed one-way or two-way ANOVA. Significance was set at $P < 0.05$, with significance levels denoted as $^{*}P < 0.05$, $^{**}P < 0.01$, and $^{***}P < 0.001$. Non-significant differences are marked as "ns."

ACKNOWLEDGMENTS

The recombinant PRRSV strain rTA-Gluc2 (54) was generously provided by Prof. Yanhua Li (Yangzhou University, China). We also extend our thanks to Prof. Liwei Li (Shanghai Veterinary Research Institute, CAAS, China) for providing anti-PRRSV-nsp10 antibody and to Prof. Lei Zhou (China Agricultural University, China) for providing anti-PRRSV-nsp2 antibody.

This work was supported by the National Key Research and Development Program of China (2023YFD1801500), the Basic and Applied Basic Research Foundation of Guangdong Province (2024A1515012991), the Science and Technology Planning Project of Guangzhou (2023B03J0947 and 2025D04J0072), and the Laboratory of Lingnan Modern Agriculture Project (NG2022003).

Y.C.: Conceptualization, Data curation, Investigation, Methodology, Validation, Visualization, and Writing-original draft; J.W. and H.L.: Data curation, Investigation, Methodology, and Validation; Z.C. and B.H.: Data curation, and Validation; C.G.: Conceptualization, Funding acquisition, Supervision, and Writing-review & editing.

AUTHOR AFFILIATION

[1]Guangdong Laboratory for Lingnan Modern Agriculture, State Key Laboratory of Animal Disease Control and Prevention, Key Laboratory of Zoonosis Prevention and Control of Guangdong Province, College of Veterinary Medicine, South China Agricultural University, Guangzhou, Guangdong, People's Republic of China

AUTHOR ORCIDs

Chunhe Guo http://orcid.org/0000-0002-7859-1985

AUTHOR CONTRIBUTIONS

Yongjie Chen, Conceptualization, Data curation, Investigation, Methodology, Validation | Jingxing Wang, Data curation, Investigation, Methodology, Validation | Haotong Lu, Data curation, Investigation, Methodology, Validation | Zishen Chen, Data curation, Validation | Baoying Huang, Data curation, Validation | Chunhe Guo, Conceptualization, Supervision

Downloaded from https://journals.asm.org/journal/jvi on 25 February 2026 by 147.162.241.196.

DATA AVAILABILITY

All data are available in the figures or can be provided upon request.

ADDITIONAL FILES

The following material is available online.

Supplemental Material

Table S1 (JVI02121-25-s0001.docx). Primer sequences used in this study.

REFERENCES

1. VanderWaal K, Deen J. 2018. Global trends in infectious diseases of swine. Proc Natl Acad Sci USA 115:11495–11500. https://doi.org/10.1073/pnas.1806068115
2. Kamel M, Aleya S, Almagharbeh WT, Aleya L, Abdel-Daim MM. 2025. The emergence of highly pathogenic avian influenza H5N1 in dairy cattle: implications for public health, animal health, and pandemic preparedness. Eur J Clin Microbiol Infect Dis 44:1817–1833. https://doi.org/10.1007/s10096-025-05147-z
3. Osemeke O, Silva GS, Corzo CA, Kikuti M, Vadnais S, Yue X, Linhares D, Holtkamp D. 2025. Economic impact of productivity losses attributable to porcine reproductive and respiratory syndrome virus in United States pork production, 2016-2020. Prev Vet Med 244:106627. https://doi.org/10.1016/j.prevetmed.2025.106627
4. Tu T, Li Y, Zhang G, Du C, Zhou Y, Jiang D, Luo Y, Yao X, Yang Z, Ren M, Wang Y. 2024. Isolation, identification, recombination analysis and pathogenicity experiment of a PRRSV recombinant strain in Sichuan Province, China. Front Microbiol 15:1362471. https://doi.org/10.3389/fmicb.2024.1362471
5. Albina E. 1997. Epidemiology of porcine reproductive and respiratory syndrome (PRRS): an overview. Vet Microbiol 55:309–316. https://doi.org/10.1016/s0378-1135(96)01322-3
6. Gong B, Xu H, Sun Q, Li C, Xiang L, Zhao J, Li W, Guo Z, Li J, Wang Q, Peng J, Zhou G, Leng C, Tang YD, Wu J, Liu H, An TQ, Cai X, Tian ZJ, Zhang H. 2024. Dissecting genetic diversity and evolutionary trends of Chinese PRRSV-1 based on whole-genome analysis. Transbound Emerg Dis 2024:9705539. https://doi.org/10.1155/2024/9705539
7. Tian X, Wei Z, Khan M, Zhou Z, Zhang J, Huang X, Yang Y, Wang S, Wang H, Cai X, Meng F, An T. 2025. Refining lineage classification and updated RFLP patterns of PRRSV-2 revealed viral spatiotemporal distribution characteristics in China in 1991-2023. Transbound Emerg Dis 2025:9977088. https://doi.org/10.1155/tbed/9977088
8. Kappes MA, Faaberg KS. 2015. PRRSV structure, replication and recombination: origin of phenotype and genotype diversity. Virology (Auckl) 479–480:475–486. https://doi.org/10.1016/j.virol.2015.02.012
9. Lee YJ, Park C-K, Nam E, Kim S-H, Lee O-S, Lee DS, Lee C. 2010. Generation of a porcine alveolar macrophage cell line for the growth of porcine reproductive and respiratory syndrome virus. J Virol Methods 163:410–415. https://doi.org/10.1016/j.jviromet.2009.11.003
10. Huang B, Deng L, Xu T, Jian Z, Lai S, Ai Y, Xu Z, Zhu L. 2024. Isolation and pathogenicity comparison of two novel natural recombinant porcine reproductive and respiratory syndrome viruses with different recombination patterns in Southwest China. Microbiol Spectr 12:e0407123. https://doi.org/10.1128/spectrum.04071-23
11. Li H, Zhang R, Xie H, Zhou Y, Wang X. 2025. Key amino acids in RNA polymerase and helicase proteins regulate RNA synthesis efficiency in porcine reproductive and respiratory syndrome virus. J Biol Chem 301:110247. https://doi.org/10.1016/j.jbc.2025.110247
12. He Z, Yan J, Liu M, Liao J, Li F, Guo C. 2025. Host innate immune antagonism and immune evasion strategies of porcine reproductive and respiratory syndrome virus. Int J Biol Macromol 322:146756. https://doi.org/10.1016/j.ijbiomac.2025.146756
13. He Z, Li F, Liu M, Liao J, Guo C. 2025. Porcine reproductive and respiratory syndrome virus: challenges and advances in vaccine development. Vaccines (Basel) 13:260. https://doi.org/10.3390/vaccines13030260
14. Zhu J, Lai Y, Cheng M, Dash RC, Guo S, Guo J, Su Y, Wolek A, Issacs B, Liu Z, Li Q, Mishra N, Garmendia A, Hadden MK, Tian XC, He X, Tang Y. 2025. Discovery of small molecules against porcine reproductive and respiratory syndrome virus replication by targeting NendoU activity. J Virol 99:e0203424. https://doi.org/10.1128/jvi.02034-24
15. Wang H, Pei R, Li X, Deng W, Xing S, Zhang Y, Zhang C, He S, Sun H, Xiao S, Xiong J, Zhang Y, Chen X, Wang Y, Guo Y, Zhang B, Shang L. 2022. The structure-based design of peptidomimetic inhibitors against SARS-CoV-2 3C like protease as potent anti-viral drug candidate. Eur J Med Chem 238:114458. https://doi.org/10.1016/j.ejmech.2022.114458
16. Zhu X, Gao X, Wu Y, Lu J, Chen X, Zhao C, Li H, Zhang Z, Liu S, Xiao G, Pan X. 2025. Eltrombopag, an FDA-approved drug, inhibits dengue virus type 2 by targeting NS2B-NS3 protease. Virol Sin 40:439–450. https://doi.org/10.1016/j.virs.2025.05.009
17. Wang K, Wang HQ, Yang G, Wu S, Yan HY, Wu MY, Li YH, Jiang JD. 2025. Carrimycin exhibited broad spectrum inhibitory activities against coronaviruses replication through down-regulating host factor TMEM41B. Acta Pharmacol Sin 46:2006–2015. https://doi.org/10.1038/s41401-025-01577-9
18. Zhu J, He X, Bernard D, Shen J, Su Y, Wolek A, Issacs B, Mishra N, Tian X, Garmendia A, Tang Y. 2023. Identification of new compounds against PRRSV infection by directly targeting CD163. J Virol 97:e0005423. https://doi.org/10.1128/jvi.00054-23
19. Wu CY, Satapati S, Gui W, Wynn RM, Sharma G, Lou M, Qi X, Burgess SC, Malloy C, Khemtong C, Sherry AD, Chuang DT, Merritt ME. 2018. A novel inhibitor of pyruvate dehydrogenase kinase stimulates myocardial carbohydrate oxidation in diet-induced obesity. J Biol Chem 293:9604–9613. https://doi.org/10.1074/jbc.RA118.002838
20. Tso SC, Qi X, Gui WJ, Wu CY, Chuang JL, Wernstedt-Asterholm I, Morlock LK, Owens KR, Scherer PE, Williams NS, Tambar UK, Wynn RM, Chuang DT. 2014. Structure-guided development of specific pyruvate dehydrogenase kinase inhibitors targeting the ATP-binding pocket. J Biol Chem 289:4432–4443. https://doi.org/10.1074/jbc.M113.533885
21. Narayan R, Sharma M, Yadav R, Biji A, Khatun O, Kaur S, Kanojia A, Joy CM, Rajmani R, Sharma PR, Jeyasankar S, Rani P, Shandil RK, Narayanan S, Rao DC, Satchidanandam V, Das S, Agarwal R, Tripathi S. 2023. Picolinic acid is a broad-spectrum inhibitor of enveloped virus entry that restricts SARS-CoV-2 and influenza A virus *in vivo*. Cell Rep Med 4:101127. https://doi.org/10.1016/j.xcrm.2023.101127
22. Gao J, Xiao S, Liu X, Wang L, Zhang X, Ji Q, Wang Y, Mo D, Chen Y. 2014. Inhibition of HSP90 attenuates porcine reproductive and respiratory syndrome virus production *in vitro*. Virol J 11:17. https://doi.org/10.1186/1743-422X-11-17
23. Zhang S, Wang P, Hu B, Liu W, Lv X, Chen S, Shao Z. 2021. HSP90 inhibitor 17-AAG attenuates nucleus pulposus inflammation and catabolism induced by M1-polarized macrophages. Front Cell Dev Biol 9:796974. https://doi.org/10.3389/fcell.2021.796974
24. Gao F, Li P, Yin Y, Du X, Cao G, Wu S, Zhao Y. 2023. Molecular breeding of livestock for disease resistance. Virology (Auckl) 587:109862. https://doi.org/10.1016/j.virol.2023.109862
25. Wang S, Tian W, Pan D, Liu L, Xu C, Ma Y, Wang D, Jiang L. 2022. A comprehensive analysis of the myocardial transcriptome in ZBED6-knockout bama Xiang pigs. Genes (Basel) 13:1382. https://doi.org/10.3390/genes13081382
26. Ren Z, Kang P, Zhang P, Sun C, Chen J, Xiang H, Luo S, Cai R, Huang Y, Jin Y, Wang G, Wang X. 2025. Development of SYBR green I-based real-time qPCR differential diagnosis assays for porcine reproductive and respiratory syndrome virus typing in Guangdong province. Front Vet Sci 12:1495128. https://doi.org/10.3389/fvets.2025.1495128

Downloaded from https://journals.asm.org/journal/jvi on 25 February 2026 by 147.162.241.196.

27. Xu H, Liu Z, Zheng S, Han G, He F. 2020. CD163 antibodies inhibit PRRSV infection via receptor blocking and transcription suppression. Vaccines (Basel) 8:592. https://doi.org/10.3390/vaccines8040592
28. Hsueh FC, Wang SY, Lin WH, Lin CF, Tsai CY, Huang CW, Sun N, Chiou MT, Lin CN. 2021. Correlation of neutralizing antibodies (NAbs) between sows and piglets and evaluation of protectability associated with maternally derived NAbs in pigs against circulating porcine reproductive and respiratory syndrome virus (PRRSV) under field conditions. Vaccines (Basel) 9:414. https://doi.org/10.3390/vaccines9050414
29. Zheng Y, Ling M, Feng J, Yu Y, Song M, Tao Y, Zhang A, Wang X. 2025. Inhibition of PRRSV replication by fangchinoline and cepharanthine from medicinal herbs through targeting of the CD163 protein. Vet Microbiol 306:110536. https://doi.org/10.1016/j.vetmic.2025.110536
30. Wang T, Chen L, Wang A, Xu Y, Zhang Y, Zhao Q, Ren Q, Liu S, Li L, Li Y, Wu J. 2025. Hyperoside inhibits PRRSV proliferation via the TLR4/NF-κB and p62-Nrf2-Keap1 signaling pathways, mediating inflammation and autophagy. Microbiol Spectr 13. https://doi.org/10.1128/spectrum.03107-24
31. Zhang Z, Wu W, Li Q, Du F, Wang X, Yang M, Zhang H. 2024. The effect of matrine and glycyrrhizic acid on porcine reproductive and respiratory syndrome virus *in vitro* and *in vivo*. Virol J 21:150. https://doi.org/10.1186/s12985-024-02415-w
32. Sheahan TP, Sims AC, Zhou S, Graham RL, Pruijssers AJ, Agostini ML, Leist SR, Schäfer A, Dinnon KH III, Stevens LJ, et al. 2020. An orally bioavailable broad-spectrum antiviral inhibits SARS-CoV-2 in human airway epithelial cell cultures and multiple coronaviruses in mice. Sci Transl Med 12:eabb5883. https://doi.org/10.1126/scitranslmed.abb5883
33. Yan H, Li H, Chen X, Wang J, Yang J, Xu Z, Hao C, Wang W. 2025. Salvianolic acid A acts as a herpes simplex virus dual inhibitor by blocking glycoprotein B-mediated adsorption and membrane fusion. Phytomedicine 143:156910. https://doi.org/10.1016/j.phymed.2025.156910
34. Amona FM, Pang Y, Gong X, Wang Y, Fang X, Zhang C, Chen X. 2024. Mechanism of PRRSV infection and antiviral role of polyphenols. Virulence 15:2417707. https://doi.org/10.1080/21505594.2024.2417707
35. Zhang X, Chen Y, Liu M, Long X, Guo C. 2024. Intervention strategies targeting virus and host factors against porcine reproductive and respiratory syndrome virus: a systematic review. Int J Biol Macromol 279:135403. https://doi.org/10.1016/j.ijbiomac.2024.135403
36. Li Y, Zheng X, Xie L, Kapustina M, Shirasaki T, Yonish B, Chen X, Hirai-Yuki A, Nagata N, Suzuki R, Isogawa M, Vogt MR, Muramatsu M, Lemon SM. 2025. Heat shock protein 90 chaperone activity is required for hepatitis A virus replication. J Virol 99:e0050225. https://doi.org/10.1128/jvi.00502-25
37. Su G, Su L, Luo D, Yang X, Liu Z, Lin Q, An T, Weng C, Chen W, Zeng Z, Chen J. 2024. Cepharanthine inhibits African swine fever virus replication by suppressing AKT-associated pathways through disrupting Hsp90-Cdc37 complex. Int J Biol Macromol 282:137070. https://doi.org/10.1016/j.ijbiomac.2024.137070
38. Qin S, Hu X, Lin S, Xiao J, Wang Z, Jia J, Song X, Liu K, Ren Z, Wang Y. 2021. Hsp90 inhibitors prevent HSV-1 replication by directly targeting UL42-Hsp90 complex. Front Microbiol 12:797279. https://doi.org/10.3389/fmicb.2021.797279
39. Mohl BP, Roy P. 2019. Hsp90 chaperones bluetongue virus proteins and prevents proteasomal degradation. J Virol 93:e00898-19. https://doi.org/10.1128/JVI.00898-19
40. Zhu Z, Zhang X, Dong W, Wang X, He S, Zhang H, Wang X, Wei R, Chen Y, Liu X, Guo C. 2020. TREM2 suppresses the proinflammatory response to facilitate PRRSV infection via PI3K/NF-κB signaling. PLoS Pathog 16:e1008543. https://doi.org/10.1371/journal.ppat.1008543
41. Zhang Z, Sun D, Tang H, Ren J, Yin S, Yang K. 2023. PER2 binding to HSP90 enhances immune response against oral squamous cell carcinoma by inhibiting IKK/NF-κB pathway and PD-L1 expression. J Immunother Cancer 11:e007627. https://doi.org/10.1136/jitc-2023-007627
42. Giguère PM, Gall BJ, Ezekwe EAD Jr, Laroche G, Buckley BK, Kebaier C, Wilson JE, Ting JP, Siderovski DP, Duncan JA. 2014. G protein signaling modulator-3 inhibits the inflammasome activity of NLRP3. J Biol Chem 289:33245–33257. https://doi.org/10.1074/jbc.M114.578393
43. Radhakrishnan A, Mukherjee T, Mahish C, Kumar PS, Goswami C, Chattopadhyay S. 2023. TRPA1 activation and Hsp90 inhibition synergistically downregulate macrophage activation and inflammatory responses *in vitro*. BMC Immunol 24:16. https://doi.org/10.1186/s12865-023-00549-0
44. Zhu Z, Xu Y, Chen L, Zhang M, Li X. 2023. Bergamottin inhibits PRRSV replication by blocking viral non-structural proteins expression and viral RNA synthesis. Viruses 15:1367. https://doi.org/10.3390/v15061367
45. Xu Y, Zhu Z, Zhang M, Chen L, Tian K, Li X. 2024. Tubercidin inhibits PRRSV replication via RIG-I/NF-κB pathways and interrupting viral nsp2 synthesis. Microbiol Spectr 12:e0347923. https://doi.org/10.1128/spectrum.03479-23
46. Yang C, Lu K, Wang J, Su H, Cheng L, Nong C, Pan X, Li H, Peng Z, Chen Y, Wu Y, Ma Q, Hu G, Liu S. 2025. Dihydrotanshinone I targets the spike N-terminal domain to inhibit SARS-CoV-2 entry and spike-induced inflammation. Phytomedicine 145:156989. https://doi.org/10.1016/j.phymed.2025.156989
47. Zheng Y, Zhang H, Luo Q, Sha H, Li G, Mu X, He Y, Kong W, Wu A, Zhang H, Yu X. 2023. Research progress on NSP11 of Porcine reproductive and respiratory syndrome virus. Vet Sci 10:451. https://doi.org/10.3390/vetsci10070451
48. Xu L, Zhou L, Sun W, Zhang P, Ge X, Guo X, Han J, Yang H. 2018. Nonstructural protein 9 residues 586 and 592 are critical sites in determining the replication efficiency and fatal virulence of the Chinese highly pathogenic porcine reproductive and respiratory syndrome virus. Virology (Auckl) 517:135–147. https://doi.org/10.1016/j.virol.2018.01.018
49. Diao F, Bai J, Jiang C, Sun Y, Gao Y, Nauwynck H, Jiang P, Liu X. 2023. The papain-like protease of porcine reproductive and respiratory syndrome virus impedes STING translocation from the endoplasmic reticulum to the golgi apparatus by deubiquitinating STIM1. J Virol 97:e0018823. https://doi.org/10.1128/jvi.00188-23
50. Nan H, Lan J, Tian M, Dong S, Tian J, Liu L, Xu X, Chen H. 2018. The network of interactions among porcine reproductive and respiratory syndrome virus non-structural proteins. Front Microbiol 9:970. https://doi.org/10.3389/fmicb.2018.00970
51. Lian W, Jang J, Potisopon S, Li PC, Rahmeh A, Wang J, Kwiatkowski NP, Gray NS, Yang PL. 2018. Discovery of immunologically inspired small molecules that target the viral envelope protein. ACS Infect Dis 4:1395–1406. https://doi.org/10.1021/acsinfecdis.8b00127
52. Pitts J, Hsia CY, Lian W, Wang J, Pfeil MP, Kwiatkowski N, Li Z, Jang J, Gray NS, Yang PL. 2019. Identification of small molecule inhibitors targeting the zika virus envelope protein. Antiviral Res 164:147–153. https://doi.org/10.1016/j.antiviral.2019.02.008
53. Huang GG, Wang HY, Wang XH, Yang T, Zhang XM, Feng CL, Zhao WM, Tang W. 2024. Atranorin inhibits zika virus infection in human glioblastoma cell line SNB-19 via targeting zika virus envelope protein. Phytomedicine 125:155343. https://doi.org/10.1016/j.phymed.2024.155343
54. Li Y, Ren C, Li C, Xiao Y, Zhou Y. 2022. A recombinant porcine reproductive and respiratory syndrome virus stably expressing a Gaussia luciferase for antiviral drug screening assay and luciferase-based neutralization assay. Front Microbiol 13:907281. https://doi.org/10.3389/fmicb.2022.907281

Downloaded from https://journals.asm.org/journal/jvi on 25 February 2026 by 147.162.241.196.